Ecole Nationale Supérieur de l´Electronique et ses Applications

Injected Phototransistor Oscillator

Carlos Alberto Araújo Viana

FINAL VERSION 1.0

Internship Project Report developed in the Thales Air System in partnership with the ESYCOM Laboratory

Tutor: Julien SCHIELLIEN
Supervisor: Jean-Luc POLLEUX

September 2010

Résume

Active Electronically Scanned Array technologie est couramment utilisé dans les systèmes radar de pointe. Cela nous amène à la nécessité de distribuer des signaux RF d'une grande pureté spectrale, horloges et oscillateurs locaux, du synthétiseur vers un ensemble de modules répartis sur la surface du radar.

La réalisation de cette distribution par fibre optique constitue un challenge technologique majeur pour la nouvelle génération de systèmes de radar. Avec cette distribution optique, nous devons utiliser des techniques de régénération du signal comme PLL (Phase Locked Loop) et oscillateur injecté.

L'étape prochaine consiste à fusionner les modules de distribution et de la régénération de signaux optiques pour fournir une interface compacte et compatible avec les concepts futurs de radar.

Ce projet vise dans la première partie de la modélisation d'un phototransistor à hétérojonction (HPT) avec l'aide de mesures et d'outils de simulation hyperfréquence (ADS). Dans un second temps, en s'appuyant sur le modèle développé, un ou plusieurs oscillateurs à HPT seront développés et étudié en termes du bruit de phase. Parallèlement à cette étape, des mesures en bruits de phase sur une série de HPT seront réalisées afin de mener à bien les simulations en bruit de phase sur le circuit d'oscillateur.

Abstract

Active Electronically Scanned Array (AESA) technology is commonly used in advanced radar systems. This brings us to the need to distribute RF signals with high spectral purity, including clock signals and local oscillators.

The realization of this distribution through the fiber optic technology is a major challenge for new generations of radar systems. With this optical distribution we need to use signal regeneration techniques like PLL (Phase Locked Loop) and Injected Oscillator.

The next step is to integrate the distribution modules and optical signal regeneration to provide a compact interface and compatible with the concepts of future radars.

This project aims in the first part of modelling a Heterojunction Phototransistor (HPT) with the help of measurements and microwave simulation tool (ADS). Second part develops a study taking into account the phase noise of one or more oscillators integrating the HPT model. In parallel to this second step, phase noise measurements of a series of HPT will be conducted in order to perform simulations in the oscillator circuit.

Resumo

Os sistemas avançados de radar usam antenas activas para procederem ao varrimento electrónico. Isto leva-nos à necessidade de distribuir sinais de radiofrequência de elevada pureza espectral, nomeadamente sinais de relógio e osciladores locais.

A realização desta distribuição através da tecnologia da fibra óptica constitui um grande desafio para as novas gerações de sistemas de radar. Nesta distribuição óptica são utilizadas técnicas de regeneração de sinal como PLL – Phase Locked Loop e Osciladores Injectados.

A próxima etapa prende-se em integrar os módulos de distribuição óptica e de regeneração de sinal para oferecer uma interface compacta e compatível com os conceitos de radar futuro.

Este projecto procura numa primeira parte de modelizar um Phototransistor de Heterojunção (HPT), com a ajuda de medições e ferramentas de simulação microondas (ADS). Em segundo desenvolver um estudo tendo em conta o ruído de fase de um ou vários osciladores a HPT apoiado pelo modelo desenvolvido. Paralelamente a esta segunda etapa, medições de ruído de fase de uma serie de HPT serão realizadas a fim de realizar simulações no circuito do oscilador.

CONTENTS

List of figures

List of tables

List of acronyms and abbreviations

ADS	*Advanced Design System*
AESA	*Active Electronically Scanned Array*
AG	*Auxiliary Generator*
DOILO	*Direct Optical Injection Locked Oscillator*
EP	*Equilibrium Points*
HB	*Harmonic Balance*
HPT	*Heterojunction Phototransistor*
IFF	*Identification Friend or Foe*
IOILO	*Indirect Optical Injection locked Oscillator*
PA	*Power Amplifier*
PESA	*Passive Electronically scanned array*
PLL	*Phased Locked Loop*
SDD	*Symbolically Defined Device*
WDM	*wavelength Division Multiplexing*

Chapter 1

Introduction

This chapter intends to present an overview of the work for this dissertation, exposing the subject, describing its objectives and finally giving the presentation of the report structure.

1.1 Subject and Context

An Electronically Scanned Antenna is a type of antenna which can vary the direction or the shape of its pattern without physical displacement of its aperture. In certain advanced radar systems, such as electronic scanning is used to concentrate the beam onto specific targets or to switch rapidly from one target to another. Figure 1.1 shows a complete circuit of an Electronically Scanned Antenna in an advanced radar system. Here we can see that the antenna is composed by numerous small transmit/receive modules fed by an optical distribution network.

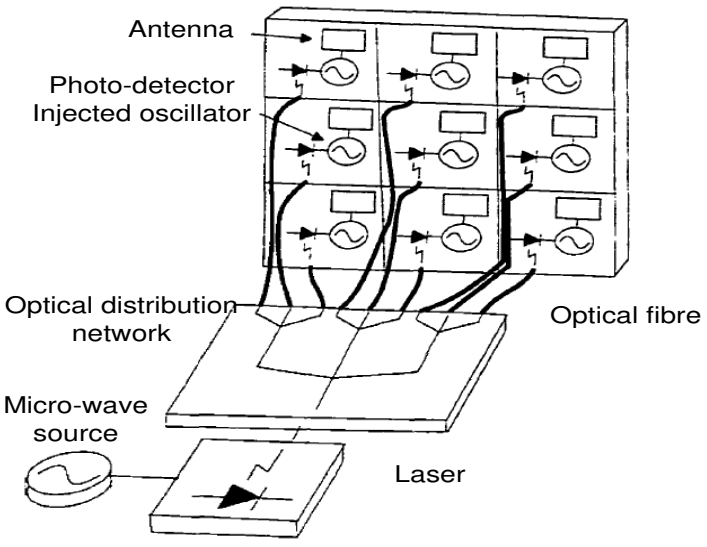

Figure 1.1 - Complete advanced radar system

In a Passive Electronically Scanned Array (PESA), the microwave feed network at the back of the antenna is powered by a single RF source, sending its waves into phase shift modules. An Active Electronically Scanned Array (AESA), instead, has an individual RF source for each of its many T/R elements, making them "active". Basically each of the T/R modules has a phase shifter, then, beams are formed by shifting the phase of the signal emitted from each radiating element, to provide constructive/destructive interference allowing the signal reinforcement in a desired direction and suppression in undesired directions.

But here we arrive to the important need of a reference signal that must be distributed to all modules. This signal has to be very precise with a high spectral purity. Radar systems continue to demand greater resolution of targets. This puts higher requirements for spectral purity on local oscillators/signal generators. For example, radar wants to detect a slow moving surface vehicle. They must detect very low level return signals, which have very small Doppler shifts. Figure 1.2 shows the radar antenna signal spectrum and the smaller Doppler-shifted return from the moving vehicle. It also shows the effect of phase noise on the return signal. It will mask out the return or smaller signal.

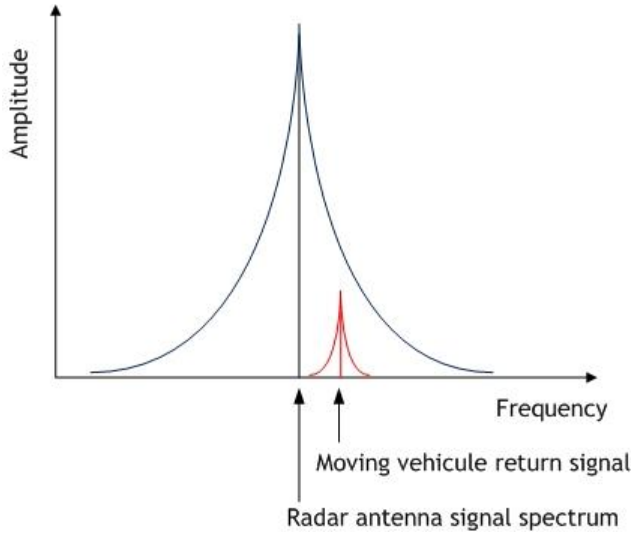

Figure 1.2 – Doppler-shift effect

Phase noise is a key element in many communication systems as it can significantly affect the performance of the systems. In an ideal world we have perfect signals with no phase noise, which means single frequency. This is not the case.

As we note in the Figure 1.1 an optical distribution network is used which gives some interesting characteristics result from the use of optical fiber like:

- Insensitive to electromagnetic interference
- Extremely low attenuation
- Bandwidth
- Using wavelength Division Multiplexing (WDM)

Signal regeneration techniques were developed to minimize the phase noise. Phased locked loop (PLL) is one of them that have been used largely. Despite good results it is composed by several active circuits that introduce noise at low frequencies. Even with a high

efficiency, it is a complex circuit which consumes lot of space. More recent, another technique was developed – Oscillator Injection. With an Oscillator Injection we have a limited number of active circuits. Therefore we get better performance of phase noise at low and high frequencies and we have a more compact circuit. This dissertation will be developed around this technique. Two ways to inject the signal in the oscillator are possible: Indirect Optical Injection locked Oscillator (IOILO) and Direct Optical Injection Locked Oscillator (DOILO).

With Indirect injection, the oscillator injected signals come from the optical network using a photodiode, matching block and amplifier block. On the other hand, with Direct Injection, a Heterojunction Phototransistor (HPT) plays the role of the photodiode and the amplifier, eliminating the matching block.

1.2 Objectives

The main goal of this dissertation is to take an indirect-OILO and replace the indirect injection, using a photodiode as the detection block, by a direct injection, using a HPT. But to arrive here an Injected Phototransistor Oscillator simulation model has to be developed which gives us the possibility to make all kind of simulations in ADS. Then some targets must be met which will be cited by topics:

- Make an amplifier model in ADS to use in Oscillators, taking into account the nonlinearities of the amplifier and phase noise.
- Validate the amplifier model used in oscillator circuit and verify the Lesson effect (1).
- Add an injected signal in this model and simulate kurokawa effect (2).
- Make a HPT model by adding an optical input verify injection effects.
- Use HPT model in the oscillator doing phase noise simulations.
- Find the best characteristics of the model changing the different parameters and design a electric circuit to implement a injected phototransistor oscillator

1.3 Dissertation structure

This document is organized according to the following structure. The current chapter is an introduction to this dissertation. In chapter 2, an introductory insight is given into the Injection Oscillator signal regeneration technique. Chapter 3 provides a study of a low noise oscillator and develops of a simulation model. Thus, a detailed study will be done in order to acquire knowledge in nonlinear dynamics of electronic circuits. Chapter 4 aims at replacing the oscillator model used in the last chapter with an injected phototransistor oscillator. At this point, the optical input will be considered.

Chapter 2

Injected Oscillator

The main objective of this first chapter is to give an introductory insight into the Injected Oscillator signal regeneration technique. Reviews some features of Free Oscillators starting by the general description of the basic operating principle and focusing in phase noise parameters.

2.1 Phase noise fundamentals

Frequency stability can be defined as the degree to which an oscillating source produces the same frequency throughout a specified period of time. Every RF and microwave source exhibits some amount of frequency instability. This can be broken down into two components - long-term and short-term stability (3). Figure 2.1 is an illustration of the two stability measurements. This thesis is primarily concerned with short-term stability, commonly referred to as phase noise.

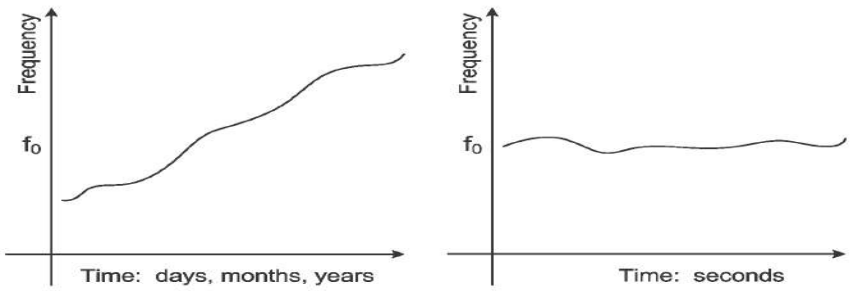

Figure 2.1 - Illustration of long-term stability (left) and short-term stability (right)

The ideal oscillator delivers a signal pure sinusoid

$$v(t) = Vo\cos(2\pi vot) \qquad \text{Eq. 1.1}$$

where Vo is the peak amplitude and vo is the carrier frequency. Let us start by reviewing some useful representations in time and frequency domain in Figure 2.2 associated with Eq.1.1

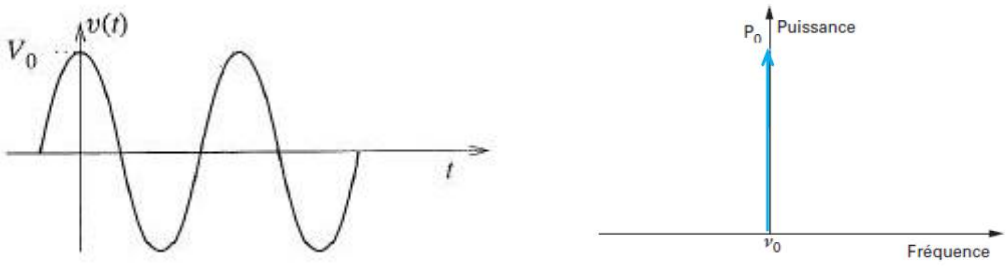

Figure 2.2 – Pure sinusoid time domain (left) and frequency domain (right)

In practice, the amplitude and frequency of real oscillators are not constant over time, see **Figure 2.3**. Various deterministic and random phenomena cause variations (drifts, modulations or fluctuations). In this section, we focus exclusively on frequency fluctuations, neglecting the variation of the amplitude.

Thus, the signal generated by an oscillator will be approximated by:

$$v(t) = Vo\cos(2\pi vot + \Delta\phi(t)) \qquad \text{Eq. 1.2}$$

where $\Delta\phi(t)$ is the phase noise. The physical dimension of $\Delta\phi(t)$ is rad.

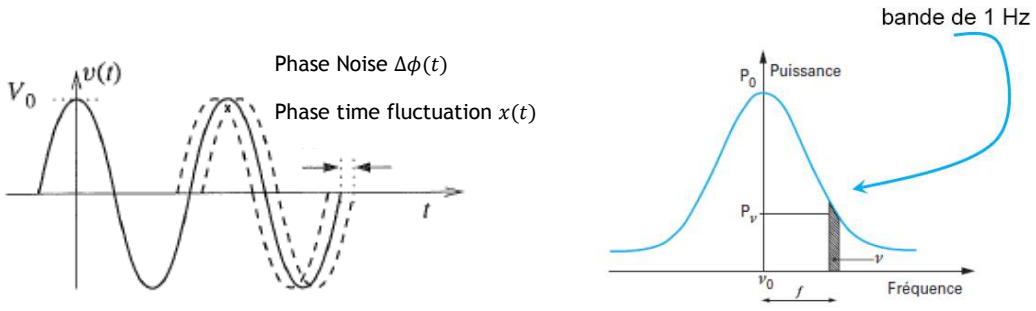

Figure 2.3 - Real sinusoid time domain (left) and frequency domain (right)

The oscillator noise is better described in terms of the power spectrum density $S_\varphi(f_m)$ of the phase noise.

$$S_\varphi(f_m) = \frac{\Delta\phi^2(t)}{BW}$$

where *BW* is the measurement bandwidth. The physical dimension of $S_\varphi(f_m)$ is $\frac{rad^2}{Hz}$.

Another useful measure of the noise energy, referred to as a single sideband (SSB) quantity, is $\mathcal{L}(f_m)$, which is then directly related to $S_\varphi(f_m)$

$$\mathcal{L}(f) = \frac{1}{2}S_\varphi(f_m) \qquad \text{Eq. 1.4}$$

As shown in Figure 2.4, we can easily know the $\mathcal{L}(f)$ with a spectrum analyzer doing the ratio of the power in one phase modulation sideband (P_{SSB}) to the total signal power (P_S) (at an offset away from the carrier). The power P_{SSB} is measured in a 1 Hz band.

$$\mathcal{L}(f_m) = \frac{P_{SSB}}{P_S}\ (^{dBc}/_{Hz}) \text{ (1.5)}$$

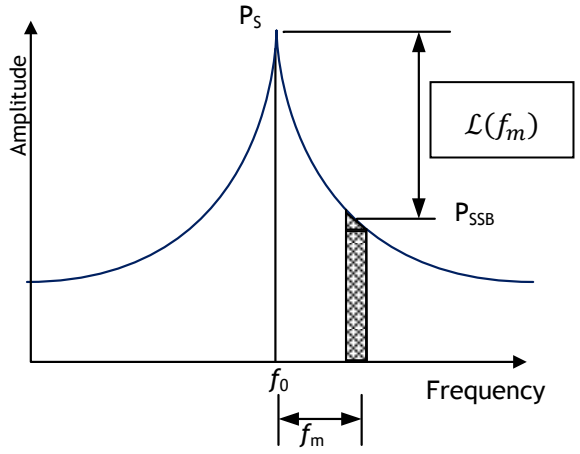

Figure 2.4 - Deriving $\mathcal{L}(f_m)$ from a spectrum analyzer display

A model that has been found almost indispensable in describing oscillator phase noise is the power-law function (Figure 2.5)

$$S_\varphi(f) = \sum_{i=-4}^{0} b_i f^i \qquad \text{Eq 1.60}$$

Phase-noise spectra are (almost) always plotted on a log-log scale, where a term f^i maps into a straight line of slope i, i.e. the slope is i x 10 dB/decade. The main noise processes and their power-law characterization are listed in Table 2.1 (4).

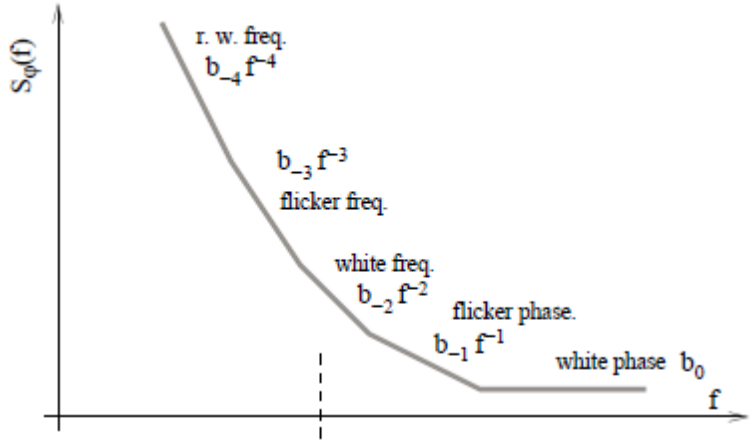

Figure 2.5 - Power spectral density (4)

In oscillators we find all the terms in Eq. 1.6 and sometimes additional terms with higher slope, while in two-port components white noise and flicker noise are the main processes.

Table 2.1 – Most frequently encountered phase-noise processes

Law	Slope	Noise Process	Units of b_i^a
$b_0 f^0$	0	White phase noise	rad^2/Hz
$b_{-1} f^{-1}$	-1	Flicker phase noise	rad^2
$b_{-2} f^{-2}$	-2	White frequency noise	$rad^2\ Hz$
$b_{-3} f^{-3}$	-3	Flicker frequency noise	$rad^2\ Hz^2$
$b_{-4} f^{-4}$	-4	Random walk of frequency	$rad^2\ Hz^3$

2.2 Phase noise in Amplifiers

Understanding amplifier phase noise is very important to the comprehension of the oscillators. We have two basic classes of noise, additive and parametric. Random noise is normally present in electronic circuits. When such noise can be represented as a voltage or current source that can be added to the signal, it is called additive noise.

When a near-dc process modulates the carrier in amplitude, in phase, or in a combination of both, it is referred to parametric noise. The most relevant difference is that additive noise is always present, while parametric noise requires nonlinearity and the presence of a carrier. Additive noise is typically constant throughout the whole frequency spectrum (white), while parametric noise can have any shape around vo, depending on the near-dc phenomenon (flicker noise) (4).

2.2.1. White Noise

The noise temperature and the noise figure, most often used in the context of amplifiers and radio receivers, are parameters that describe the white noise of a device .When the amplifier is input-terminated to a resistor at the temperature To, the equivalent spectrum density at the amplifier input is

$$N = kFTo = -174\frac{dBm}{Hz} - (NF)dB \qquad \text{Eq. 2.7}$$

where NF is noise figure (kTo = 4×10−21 J, that is, −174 dBm in 1 Hz bandwidth)

In the presence of a sinusoidal carrier of power Po, the phase noise is

$$S_{\varphi}(f) = bo = \frac{kTF}{Po} \qquad \text{Eq. } 2.8$$

2.2.2. Flicker noise

The mechanism that originates phase flickering is a low-frequency (close to dc) random process with spectrum of the flicker type that modulates the carrier (Figure 2.6).

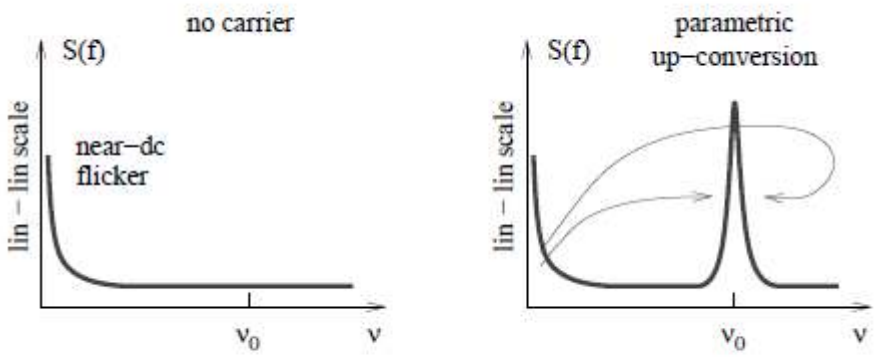

Figure 2.6 - Parametric up-conversion of near-dc flicker in amplifiers

The $^1/_f$ phase noise is best described by

$$S_\varphi(f) = b_{-1}f^{-1} \qquad \text{Eq. 2.9}$$

where the coefficient b_{-1} is an experimental parameter of the specific amplifier.

When we combine the white and flicker noise, under the assumption that they are independent we have for $S_\varphi(f)$ (see Eq. 2.8 and Eq. 2.9)

$$S_\varphi(f) = b_0 + b_{-1}\frac{1}{f} \qquad \text{Eq. 2.10}$$

$$b_0 = \frac{FkT}{P_0}$$

$$b_{-1} = constant$$

The phase-noise spectrum of an amplifier is shown in **Figure 2.7**. In this figure, we observe that the corner frequency, where the white noise equals the flicker noise, is

$$f_c = \frac{b_{-1}}{b_0} \qquad \text{Eq. 2.11}$$

Recalling that bo = FlcT/Po, the above becomes

$$f_c = \frac{b_{-1}}{FkT_0}P_0 \qquad \text{Eq. 2.12}$$

AS a relevant conclusion we can see that f_c is proportional to the carrier power P_0.

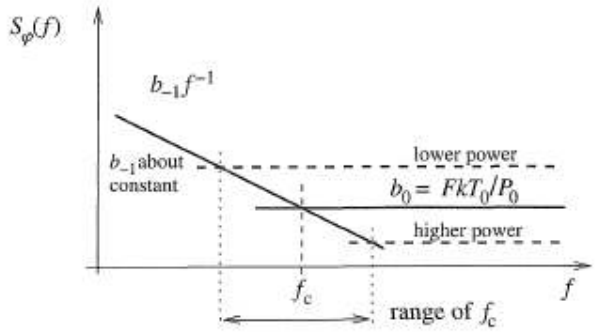

Figure 2.7 – Typical phase noise of an amplifier.

2.3 Oscillators fundamentals

Broadband noise is present everywhere in the circuit. The amplifier boosts the signal level of the noise at all frequencies. This amplified noise then travels through the feedback loop back to the input of the amplifier. The feedback loop consists of a filter that allows the signal of the desired frequency to pass. This frequency passes through the amplifier and filter repeatedly. A sinusoidal signal, centered on the frequency of the filter, begins to emerge from the noise as the signal travels around the loop many times.

The amount of positive feedback to sustain oscillation is also determined by external components.

An oscillator uses an active device, such as a diode or transistor, and a passive circuit to produce a sinusoidal steady-state RF signal. At start-up the oscillation is triggered, normally, by noise and then a properly designed oscillator will reach a stable oscillation state. This process requires that the active device would be nonlinear (4).

The combination of an amplifier with gain $A(\omega)$ and a feedback network $\beta(\omega)$, having frequency-dependent open-loop gain $H(j\omega) = \beta A$, is illustrated in

Figure 2.8.

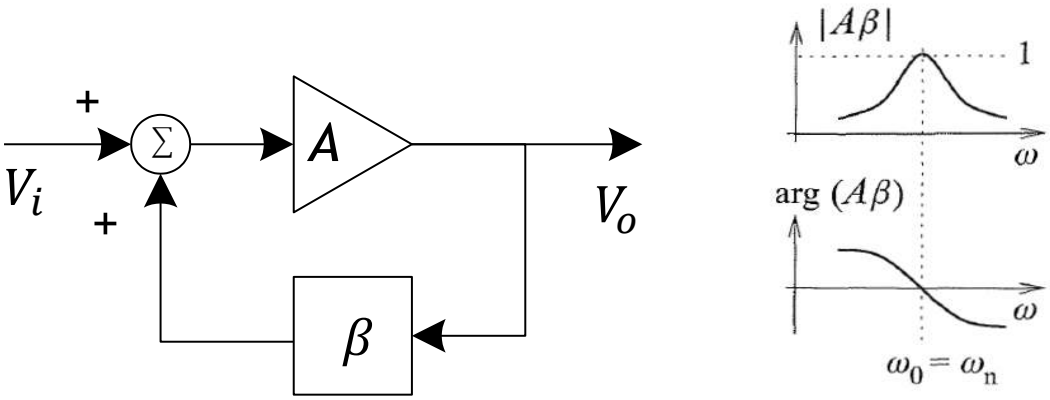

Figure 2.8 - Oscillator Model and Barkhausen conditions

The general expression for closed-loop gain is

$$H(j\omega) = \frac{V_o}{V_i} = \frac{A(\omega)}{1-\beta(\omega)A(\omega)} \qquad \text{Eq. 2.13}$$

The system will oscillate, that means output $V_o \neq 0$, even when the input signal is $V_i = 0$. This is only possible if, at $\omega = \omega_o$,

$$1 - \beta(\omega)A(\omega) = 0 \qquad \text{Eq. 2.14}$$

Thus

$$\beta(\omega)A(\omega) = 1 \text{ (Barkhausen Condition)} \qquad \text{Eq. 2.15}$$

Or equivalently

$$|\beta(\omega)A(\omega)| = 1$$
$$arg[\beta(\omega)A(\omega)] = 0º$$

At the frequency of oscillation, the total phase shift around the loop must be 0 degrees or multiples of 360 degrees, and the magnitude of the closed loop gain must be unity.

Although the model shown in

Figure 2.8 can be used to analyze and determine the necessary and sufficient conditions for oscillation, it is easier to use the model shown in Figure 2.9 where the analysis is performed in terms of a negative resistance concept. This is based on the principle that a resonator such as a crystal quartz tuned circuit, once excited, will oscillate continuously if no resistive element is present to dissipate the energy. It is the function of the amplifier to

generate the negative resistance and maintain oscillation by supplying an amount of energy equal to that dissipated.

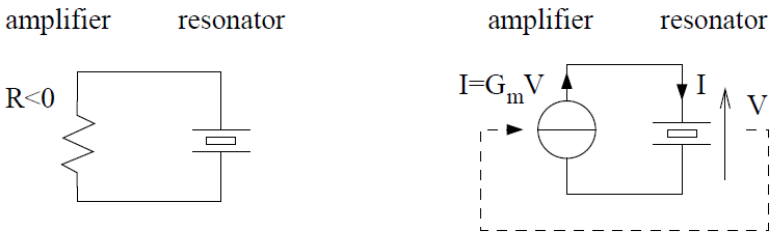

Figure 2.9 - Negative-resistance oscillator (4).

To make the oscillation grow up to the desired amplitude it is necessary that $|\beta A(j\omega)| > 1$ at $\omega = \omega_o$ for small signals (Figure 2.10). In these conditions the oscillation rises exponentially at ω_o defined by $arg[\beta A(j\omega)] = 0$. As the oscillation amplitude approaches the desired value, the nonlinearities from the amplifier reduces the loop gain. This means that the condition $|\beta(\omega)A(\omega)| = 1$ results from large-signal gain saturation.

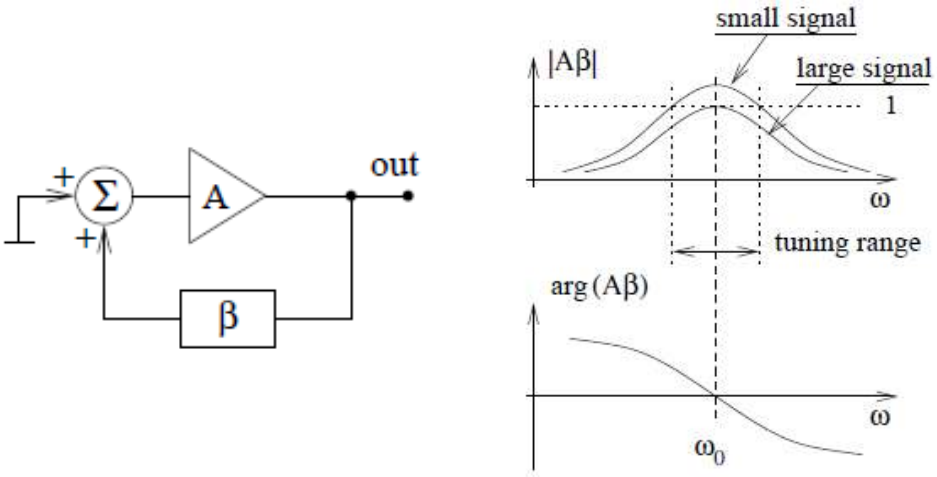

Figure 2.10 - Starting the oscillator (4)

We have two ways to adjust the desired frequency of the oscillator. The first method is pulling the natural frequency (ω_n) of the resonator by changing the parameters of the resonator's equation.

Another way to adjust the oscillation frequency (ω_o) is to introduce a static phase ψ into the loop like we can see in Figure 2.11.

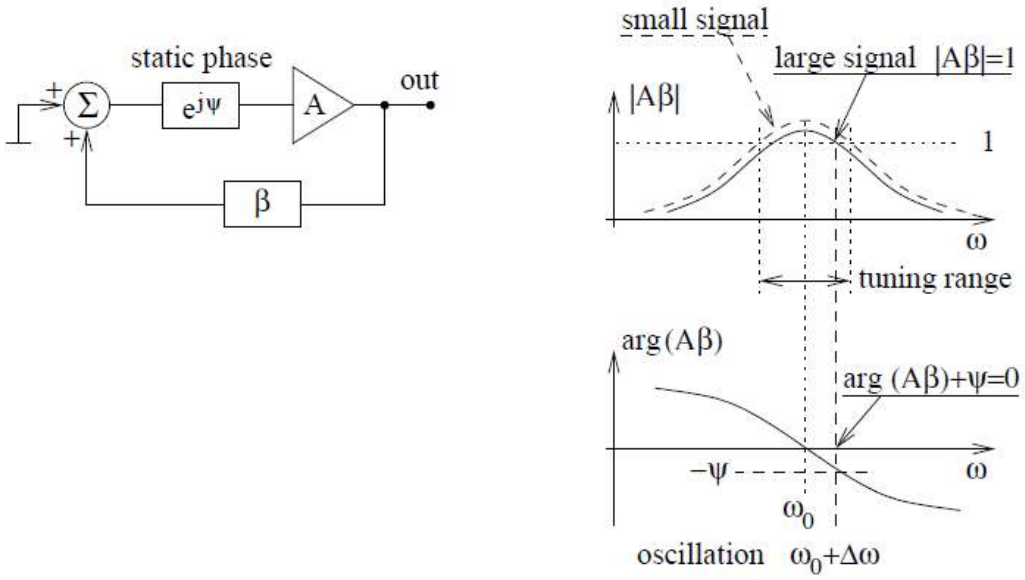

Figure 2.11 - Tuning the oscillation frequency by insertion of a static phase (4)

The barkhausen phase condition becomes

$$arg[\beta A(j\omega)] + \psi = 0º \text{ at } \omega = \omega_o$$

Thus, the loop oscillates at the frequency

$$\omega_o = \omega_n + \Delta\omega$$

2.4 Phase noise in Free Oscillators

The formula (2.4.1) was proposed by B. Leeson (1) as a model for predicting the phase noise in feedback oscillators.

$$S_\varphi(f_m) = \left[S_{\varphi\ Amplifier} + S_{\varphi\ quartz}\right].\left[1 + \frac{f_L^2}{f_m^2}\right] \qquad \text{Eq. 2.4.1}$$

where $f_L = \frac{f_0}{2.Q_L}$ is Leeson frequency and f_m is the offset frequency in Hz.

Taking the amplifier phase noise equation (2.4.2) and considering the quartz phase noise negligible

$$S_\varphi(f_m) = \left[\frac{FkT}{P_0}\left(1 + \frac{f_c}{f_m}\right)\right].\left[1 + \left(\frac{f_0}{2Q_L f_m}\right)^2\right] \qquad \text{Eq. 2.4.2}$$

One important conclusion is that the phase noise improves with both the carrier power and Q_L increasing.

Figure 2.12 shows two results when a noisy amplifier is inserted into an oscillator. For these amplifiers the phase noise is white at higher frequencies and of the flicker type below the corner frequency f_c.

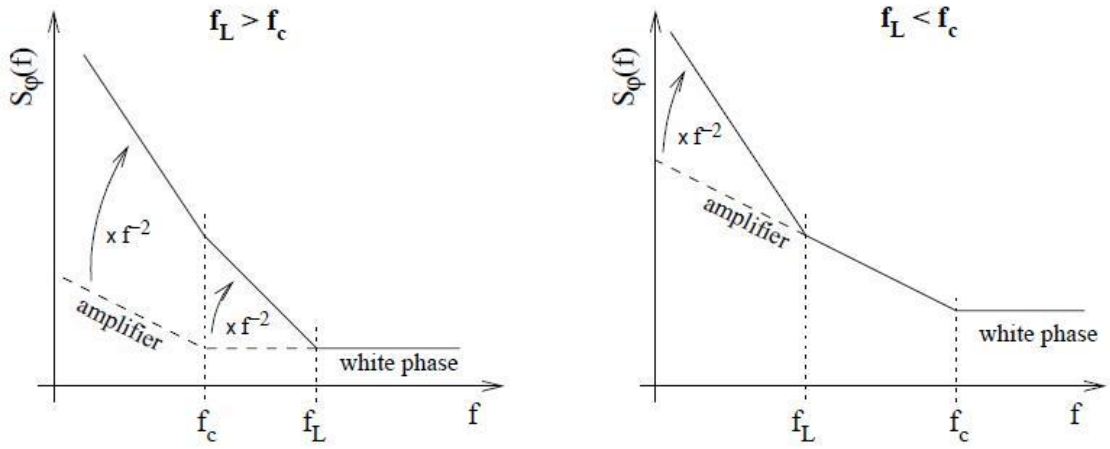

Figure 2.12 - With an amplifier phase noise, the Leeson effect yields two types of spectrum, left for $f_c < f_L$ and right for $f_c > f_L$

Both on the left and on the right we can see that at lower frequencies ($f < f_L$) the amplifier phase noise is multiplied by f^{-2}. At higher frequencies ($f > f_L$) we have the same phase noise as the amplifier.

2.5 Phase noise in Injected Oscillators

Considering the feedback oscillatory system shown in Figure 2.13 where the injection is modelled as an additive input.

The output is represented by a phase-modulated signal having a carrier frequency of ω_{inj} (rather than ω_0). In other words, the output is assumed to track the input except for a phase difference.

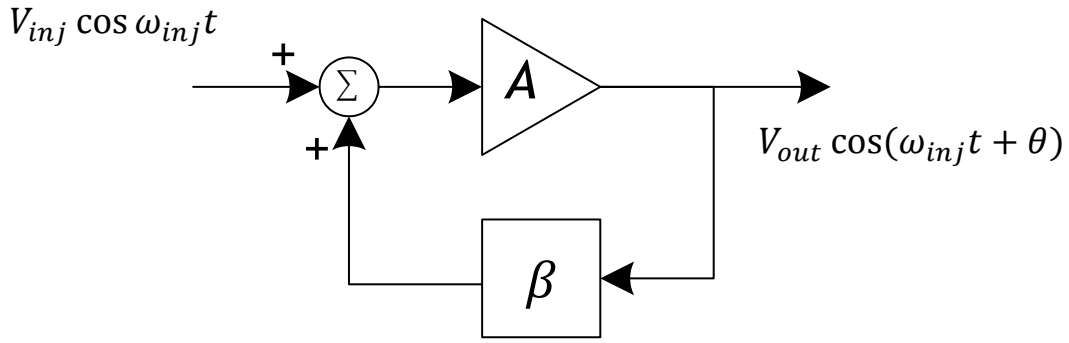

Figure 2.13 - Injected oscillator

Originally derived by Adler (5) the next equation shows us the behaviour of oscillators under injection

$$\frac{d\theta}{dt} = \omega_0 - \omega_{inj} - \frac{\omega_0}{2Q_L}.\frac{V_{inj}}{V_{out}} sin\,\theta \qquad \text{Eq. 2.5.1}$$

For the oscillator locked to the input, the phase difference, θ , must remain constant with time. Adler's equation therefore requires that

$$\frac{d\theta}{dt} = 0,$$

$$\omega_0 - \omega_{inj} - \frac{\omega_0}{2Q_L}.\frac{V_{inj}}{V_{out}} sin\,\theta = 0$$

Since $|\,sin\,\theta\,| \leq 1$, the condition for locking is

$$\left|\omega_0 - \omega_{inj}\right| \leq \frac{\omega_0}{2Q_L}.\frac{V_{inj}}{V_{out}} = \omega_{Lock}, \qquad \text{Eq. 2.5.2}$$

We can also say

$$f_{lock} = \frac{f_0}{2Q_L}.\sqrt{\frac{P_{inj}}{P_{out}}} \qquad \text{Eq. 2.5.3}$$

Where f_{lock} is the injected oscillator bandwidth, P_{inj} is the injected power at the input and P_{out} the output power of the oscillator. We have to take into account that the overall lock range is in fact $\pm f_{lock}$ around f_0. We can see in Figure 2.14 the phenomenon of injection

locking which is simply a shift in the oscillation frequency in response to the additional phase shift that arises from adding an external signal to the feedback signal.

As the oscillator output power is normally fixed by the performance requirements and f_0 is the free running frequency, Q_L and P_{inj} become the only two parameters to be optimized.

Even if taking Q_L as a tuning parameter, an inversely proportional relation between f_{lock} and f_L exists, so a compromise have to be made.

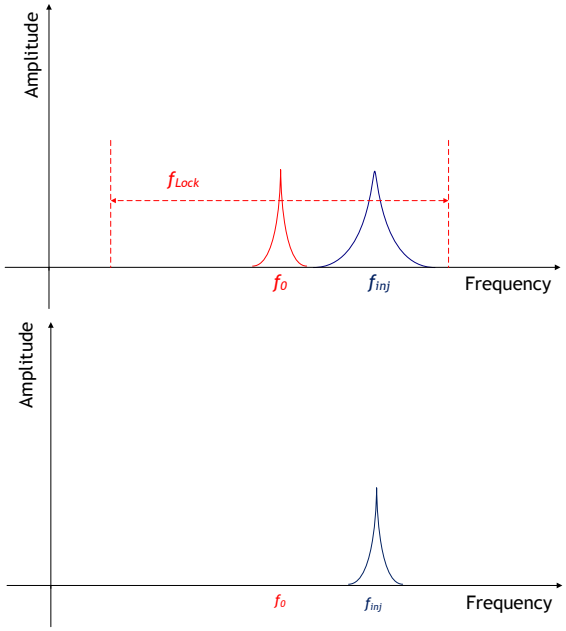

Figure 2.14 - Injection locking phenomenon

Kurokawa formula (2) allows to express the injected oscillator phase noise in function of the synchronization bandwidth f_{lock}, the free running oscillator phase noise, $S_{\varphi_{free-osc}}$, and the injected signal phase noise, $S_{\varphi_{input}}$:

$$S_{\varphi\ photo-osc} = \frac{1}{1+(\frac{f_m}{f_{lock}})^2}.S_{\varphi_{input}} + \frac{(\frac{f_m}{f_{lock}})^2}{1+(\frac{f_m}{f_{lock}})^2}.S_{\varphi_{free-osc}} \qquad \text{Eq. 2.5.4}$$

We can split the equation above into two terms, first in the left side we have input phase noise that is multiplied by a low pass band filter and in the right side a free running oscillator phase noise multiplied by a high pass filter. This means that at low frequencies, $f_m < f_{lock}$, the $S_{\varphi_{input}}$ is predominant and at higher frequencies, $f_m > f_{lock}$, the $S_{\varphi_{free-osc}}$ is predominant (Figure 2.15). We must be cautions to this conclusion as it is an empirical formula, which may find some limits.

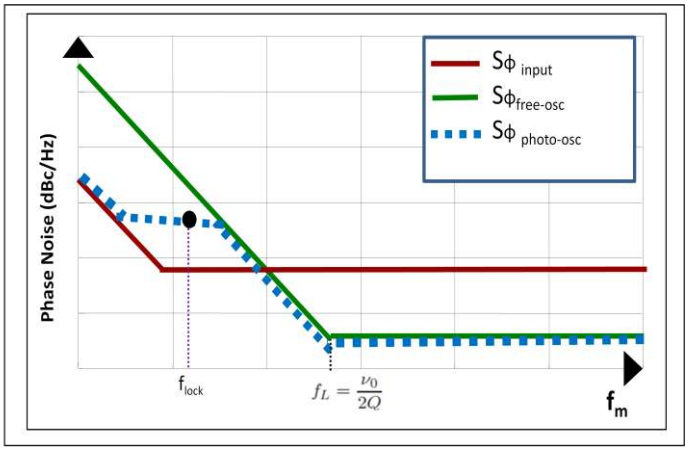

Figure 2.15 - Injected Oscillator Phase Noise

2.6 Optical Injection-Locked Oscillator (OILO)

- **Indirect OILO**

Using an optical distribution network means that an optoelectronic component must be used. In the case of an indirect injection, a photodiode acts as an optical input, having the role to convert the light signal into an electrical signal. The oscillator injected signal comes through three important blocks: detection, matching and amplification (as depicted in Figure 2.16). The matching between the photodetector is important in order to avoid the leakage of the oscillator signal into the diode.

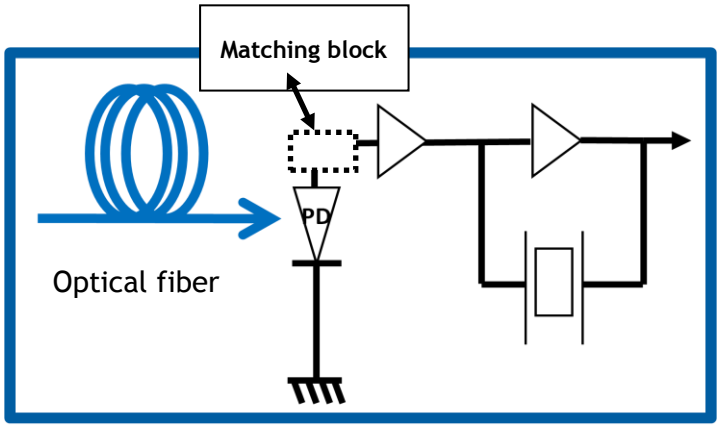

Figure 2.16 - Indirect OILO

- **Direct OILO**

Another way is to inject the signal coming from the optical network directly into the oscillator using a HPT, which is directly illuminated for synchronization as depicted in Figure 2.17. With direct injection the HPT makes the detection and amplification eliminating the need in a matching block. This type is much simpler and suitable compared with the Indirect OILO, which needs an external photodetector.

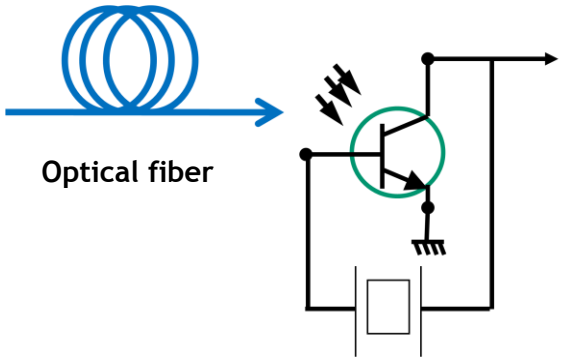

Figure 2.17 - Direct OILO

In conclusion of this chapter the Figure 2.18 show us different phase noises at different locations of the radar system using OILO.

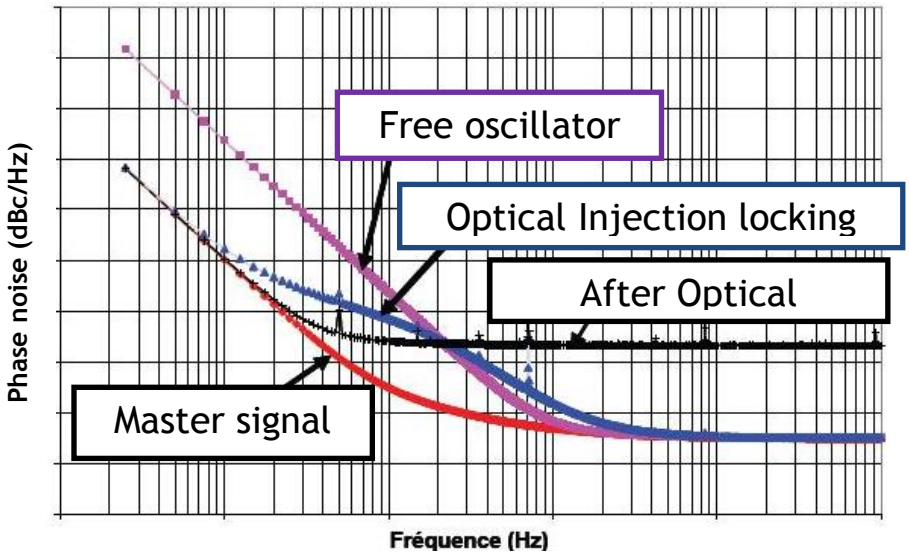

Figure 2.18 - Phase noise radar system using OILO

Chapter 3

Low Noise Oscillator

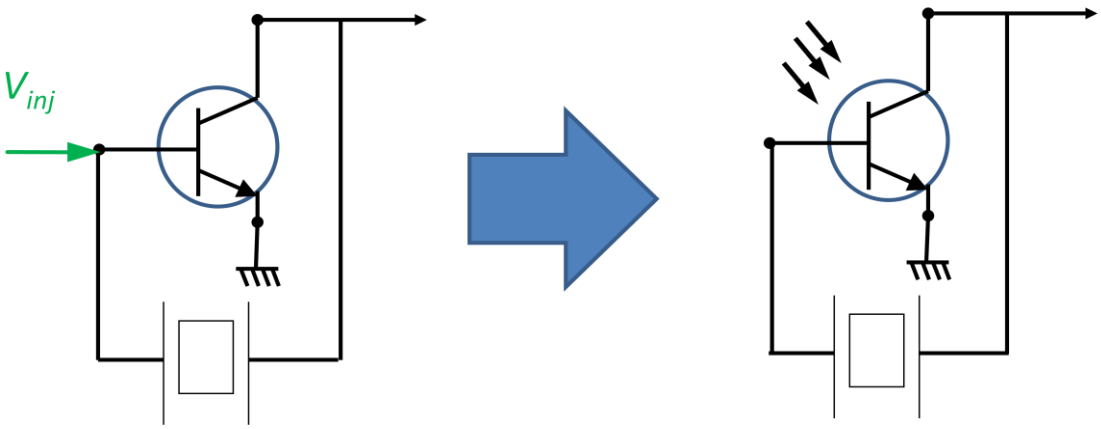

In the previous chapter, we talk about injection oscillator but first we need to know how to make a simple low noise oscillator model. Thus, a detailed study will be done in order to acquire knowledge in nonlinear dynamics of electronic circuits.

Two cases are possible in nonlinear circuits: autonomous (self-oscillating) and nonautonomous (forced) systems. The two cases will be studied in this chapter focusing on the autonomous systems. A nonlinear system solution representation will be shown: the phase-space representation.

Different simulation techniques that allow to simulate the nonlinear solutions in autonomous and synchronized circuits will be considered. The emphasis in this chapter will be on Harmonic Balance (HB) because of its efficiency when dealing with microwave systems.

After, an oscillator model will be done in ADS using a behavioural model in order to prepare the integration of the future behavioural HPT model.

3.1 State-of-the-art

Most military communication, navigation, surveillance and IFF (Identification Friend or Foe) systems that are currently under development require stable low noise oscillators for frequency control and/or timing. The best parameter to evaluate the low oscillator performance is the phase noise thus if we look in detail to the equation

$$S_{\varphi}(f_m) = \left[\frac{FkT}{P_0}\left(1+\frac{f_c}{f_m}\right)\right].\left[1+\left(\frac{f_0}{2Q_L f_m}\right)^2\right]$$

we see four parameters to be optimized, Noise Factor (F), corner frequency ($\mathrm{f_c}$), input power ($\mathrm{P_0}$) and quality factor ($\mathrm{Q_L}$). For the last decades it's been doing an effort to improve oscillator phase noise taking into account these parameters. Optimizing the three first parameters mean optimizing the design of the power amplifier. Designing a low noise oscillator is somehow the same as doing a low noise amplifier. Over the last decades, improvements in modern communication systems have driven phase noise specifications to prime importance. The technology of low phase noise signal source using crystal resonator is beginning to approach theoretical limits for a given cost, size, and power. Characteristics like the type of transistor or amplifier topology will interfere directly in the oscillator phase noise. Then we have the quality factor which is provided by the resonator and here the crystal quartz appears giving a high Q, which means better phase noise.

In the Table 3.1 we compare low noise oscillator performances provided by a some recent papers. Some conclusions are made:

- We approach to the white noise minimum -174dBc at 0 dBm output power (6).
- The favorite resonator that is used is a quartz crystal resonator which gives a really high Q factor approximately 1×10^6.
- The amplifier topology that gives the best phase noise performance, is Colpitts (Figure 3.1)
- Further optimizations like mode-selection and mode-feedback mechanism for reducing broadband and 1/f noise level have been used in circuits using crystal resonators. That not only improves the stability but also improves the phase noise performances by 10-15 dB. (7)

Table 3.1 - state-of-the-art

		(8)	(7)	(9)	(10)	(11)	(12)
Year		2009	2008	2007	2006	2004	1996
Frequency (MHz)		12.8	155.6	10	10	10	10
Phase Noise (dBc/Hz):							
	@ 1 Hz	-	-	-118	-86		-110
	@ 10 Hz	-	-120	-147	-123	-148	-140
	@ 100 Hz	-	-139	-158	-	-	-155
	@ 1 KHz	-142	160	-161	-	-	-163
	@ 10KHz	-150	-170	-162	-160		-165
	noise floor		-170	-162	-160		-170
Resonator		AT cut	VCXO	SC cut	AT-cut	AT-cut	SC-cut
	Q	-	1 M	1.3 M	-	1.2M	-
Topology		Cascode Colpitts	Colpitts	Colpitts	Colpitts	Colpitts	Colpitts
Output		-	1.93dBm	-	-	-	-
Consumption (mW)		<2.7	-	-	-	-	-

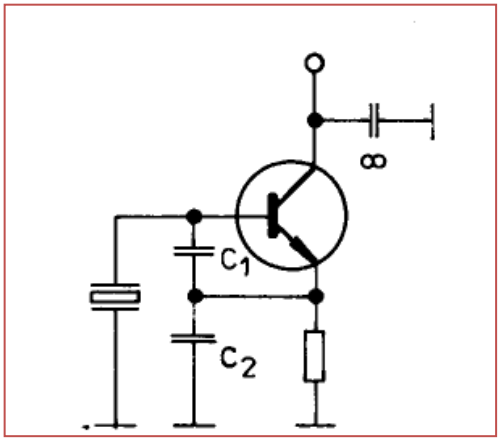

Figure 3.1 - Colpitts Crystal Oscillator

3.2 Nonlinear Simulations

Microwave circuits are often designed using nonlinear simulations techniques, like harmonic balance. Nonlinear circuits can be described by means of a system of nonlinear differential equations, (13). The nonlinear circuit's behaviour is reflected by these equations, which can be very complex. An electronic circuit can be described by a minimal set of

variables called state variables. In circuits with resistors, inductors, and capacitors, the set of state variables can be given by the capacitor voltages and the inductor currents.

The nonlinear differential equations give us the two possible cases of autonomous (self-oscillating) and nonautonomous (forced) systems. The differential equations are

$$\frac{d\bar{x}}{dt} = f(\bar{x}, t) \quad \bar{x}(t_0) = \bar{x}_0 \text{ Nonoautonomous circuit} \tag{3.2a}$$

$$\frac{d\bar{x}}{dt} = f(\bar{x}) \quad \bar{x}(0) = \bar{x}_0 \text{ Autonomous circuit} \tag{3.2b}$$

where $\bar{x}(t)$ is the system state variables vector at time t. The function f is called vector field. The dynamics of (3.2) is linear if f is linear in $\bar{x}$, otherwise, the system is nonlinear. These two cases depend on the presence or absence of time-varying generators. In the case of nonautonomous system (3.2a) f depends explicitly on time. This is the case of any forced circuit like amplifiers and mixers which has RF generator $A_{g\,cos(\omega_g t)}$ to makes time appears in the function f. Vector field is independent of time in the case of autonomous system (3.2b). Here we have free-running oscillators as examples when there are no external RF generators (only dc generators).

In an autonomous system (3.2b), it is generally possible to impose $d\bar{x}/dt = 0$ and solve $f(x) = 0$. The resulting solutions are constant solutions and are called equilibrium points (EP). These constant solutions do not exist in nonautonomous systems due to dependence on time of f. EP in autonomous circuit is the dc solution of the circuit.

A way of representing the solutions of a nonlinear system is the phase-space representation. Here we have to do a distinction between the solution curve and the solution trajectory. Figure 3.2 shows us an example of phase-space representation of a free-running oscillator (13). In the left we have a solution trajectory which is a three-dimensional space representation (current; voltage; time). Two different initial conditions have been considered for the same circuit. In the right we have a solution curve which is the same solution as the left representation but in two-dimensional space, without time axis. Autonomous system may have solution curves with two steady-state solutions: EP (dc solution- unstable) and Limit cycle (stable).

Limit cycle is the periodic solution in which the values of the system variables are repeated after exactly one period T.

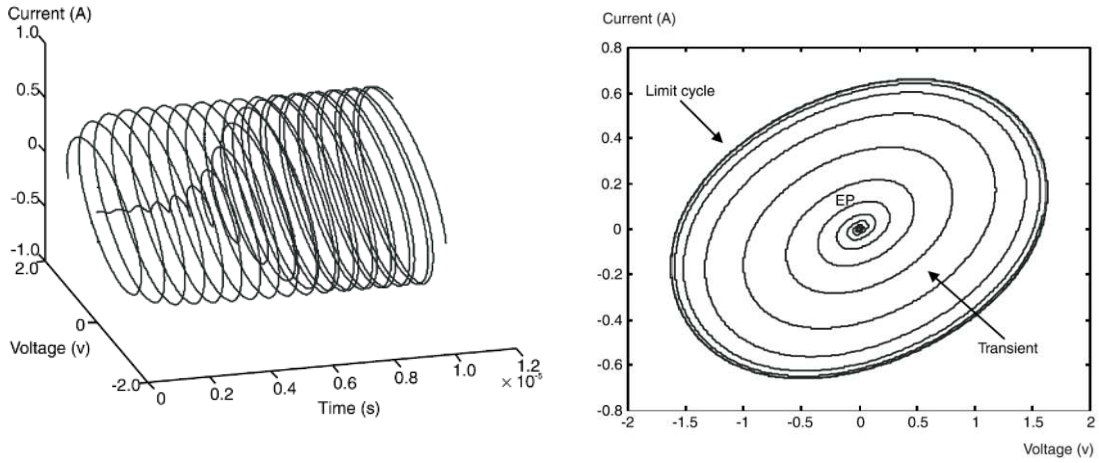

Figure 3.2 - Phase-Space representations: solution trajectory (left) and solution curve (right)

With the Harmonic Balance (HB) simulation only steady-state solutions are analyzed and may converge to either a stable or an unstable solution. This can be very difficult to do a free-running oscillator simulation which an EP always coexists with the limit cycle.

3.2.1. Harmonic Balance

Harmonic balance computes the steady state response of nonlinear circuits excited by single or multiple periodic sources. The harmonic-balance technique is an iterative technique that uses frequency-domain descriptions for the linear elements. In the case of nonlinear elements a time-domain analysis is used. Due to the employment of Fourier series expansions for the circuit variables, harmonic balance only analyzes the steady state solution (13). Then, we have the shorter simulation times compared to time-domain simulation.

Harmonic Balance uses Newton's method to solve a system of nonlinear algebraic equations, by starting with an initial guess and repeatedly solving the iteration equation. This is done until some convergence criteria are met.

Normally harmonic balance requires the insertion of an OscPort probe into the feedback loop of the oscillator or between the parts of the circuits that have negative resistance and the resonator. When inserted into the oscillator's feedback path, the OscPort performs the harmonic balance analysis of the oscillator. Specifically, we can calculate the frequency, the output power or the phase noise. The main problem when we use Oscport is the high-Q effects which lead to convergence problems and even search failures in ADS [ADS tutorial].

Harmonic Balance for Nonautonomous Circuits

The harmonic-balance technique is very efficient for the simulation of circuits in forced regime (i.e. at the fundamental frequency delivered by the input generators, such as amplifiers and mixers). However, its application to circuits with self-oscillations is more demanding. In harmonic balance, the fundamental frequency of the solution must be initially guessed. In the case of nonautonomous circuits, the independent generators deliver this fundamental frequency, so it is not a problem.

Harmonic Balance for Autonomous and Synchronized Circuits

In autonomous circuits, the disadvantage of harmonic balance, compared with time domain, comes from the necessity to fix in advance the frequency basis of the Fourier series.

Remember that in the free running oscillator circuit, aside from the periodic oscillation (limit cycle) there is always an equilibrium point (Figure 3.2). When using harmonic balance, the equilibrium point and the limit cycle constitute two different steady-state solutions to which the system may converge. However, normally convergence to the dc solution is much easier because the bias generators are forcing this solution, while at the oscillation frequency there are no forcing generators at all.

3.2.2. Auxiliary Generator Technique

We already saw that HB technique is very efficient for the nonautonomous circuit simulation. Then, auxiliary generator (AG) technique is an approach to convert the analysis of an autonomous circuit into a nonautonomous circuit which is more efficient to simulate with HB. In fact, the AG plays the role of the nonexisting generator at the autonomous frequency and forces a periodic solution, avoiding the problem of convergence to the dc point. The solution obtained with the aid of this AG must be the actual oscillator solution, and must agree with the one that would be obtained without the auxiliary generator.

In Figure 3.3 we can see that the auxiliary generator is composed by a voltage generator and an ideal filter connected in parallel at a node of the circuit.

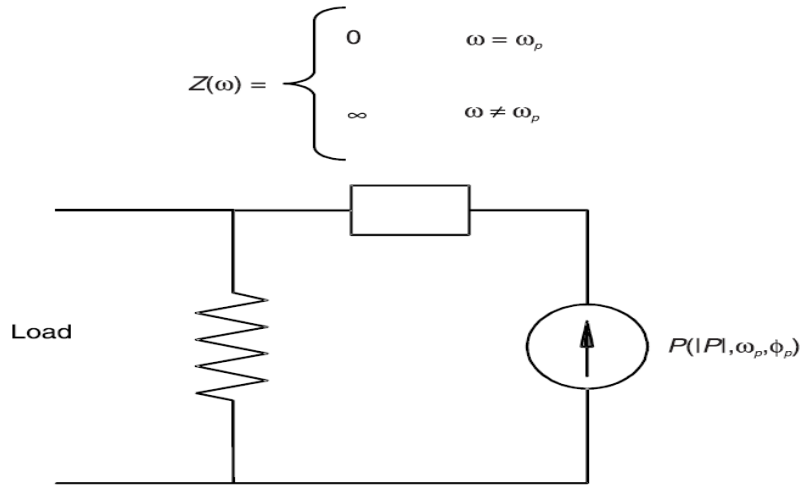

Figure 3.3 - Auxiliary Generator

To avoid a perturbation of the circuit due to the harmonic components, the voltage generator is short-circuited at frequencies different from the one delivered. So an ideal filter is necessary. Suitable locations for the auxiliary generators are the nonlinear device terminals to which feedback branches are connected, Figure 3.4 (13).

Finally, the generator may have no influence over the circuit steady-state solution. It must then have a zero current (I_{AG}) value at the delivered frequency.

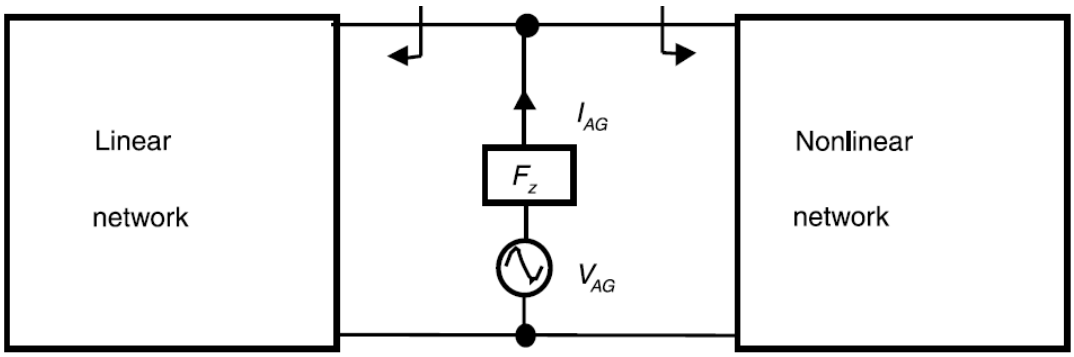

Figure 3.4 - Auxiliary Generator in an oscillator circuit (Fz is an ideal filter)

In practice, by changing the probe voltage and frequency, the solution is obtained when the probe current (I_{AG}) is zero. This means that our AG frequency and amplitude agrees with the self-oscillation frequency $\omega_{AG} \equiv \omega_0$ and amplitude $V_{AG} \equiv V_0$. Then, the fundamental frequency is delivered by the input generators therefore we can use all capabilities of the HB method.

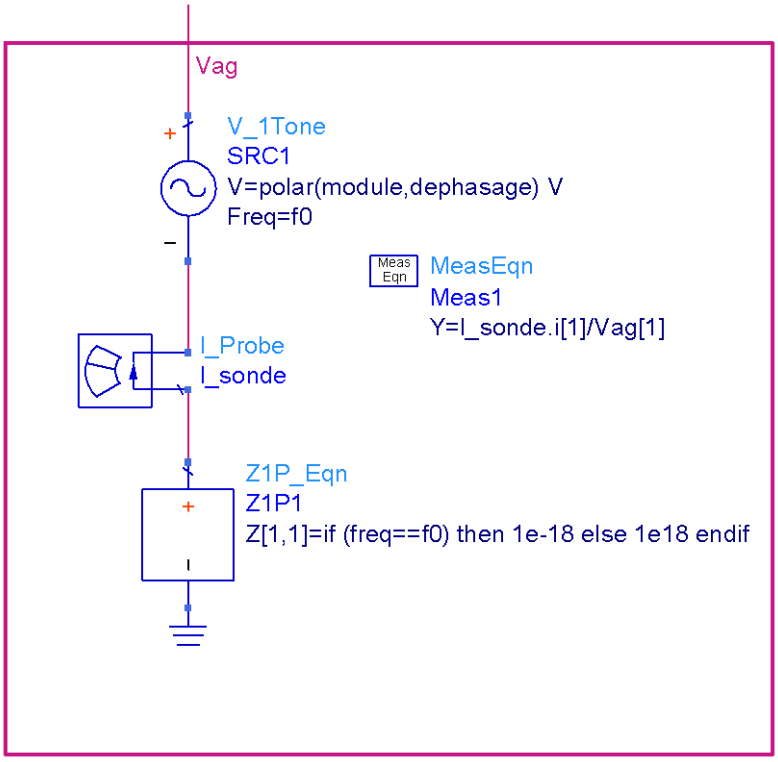

Figure 3.5 - Auxiliary Generator ADS circuit

3.3 Simulation Model

Behavioural Model

Numerous approaches of modelling PA nonlinearities have been developed in this research area to characterize the input to output complex envelope relationship (14) (15). The model forms used in identification are generally classified into three methods depending on the physical knowledge of the system: black box, grey box and white box.

- In the case of white box model the necessary priori information is all available. Are the most detailed type and more close to a full description of real device with no approximations, then, the more realistic model.
- A black box model is a system where no physical insight and prior information are available. This approach has been widely used in many research studies to predict the output of the Nonlinear Power Amplifier.
- In grey box model we are between black and white box model. Is provides a physical representation, but some of the physics is approximated.

We can see what these three models through their names are literally: in the of black box model we have a black box so we cannot see what is inside. In the white one we can see everything and in grey one we can see one part but not everything.

Figure 3.6 - Black box model

In our case a black box model will be used then no knowledge is used nor required concerning the internal circuit. This means that we don't know if we have a bipolar transistor or a field effect transistor in our circuit, for example. So the goal is having a two port network where the input and output variables relationships are described by behavioural equations. Here three important elements have to be considered in our model (Figure 3.7): Nonlinearities, Frequency Response and Phase Noise modelling.

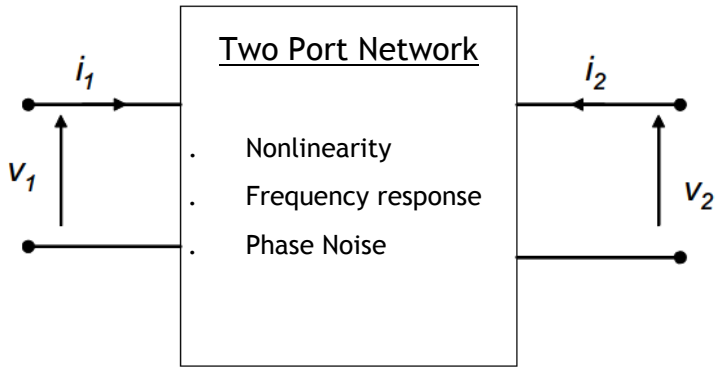

Figure 3.7 - Two port network model representation

An important tool in Advance Design System - ADS is the symbolically defined device (SDD) which enables users to specify nonlinear models directly on the circuit schematic, using algebraic relationships for the port voltages and currents (Figure 3.8). SDD can simulate both the large-signal and small-signal behaviour of a nonlinear device and can be used with any circuit simulator in ADS.

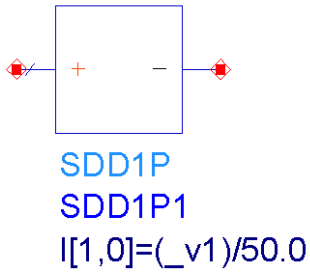

Figure 3.8 - Symbolically defined device

SDD with n port is described by n equations that relate the n port currents and the n port voltages, Figure 3.8. One important characteristic is that we can use weighting functions like for example time derivative.

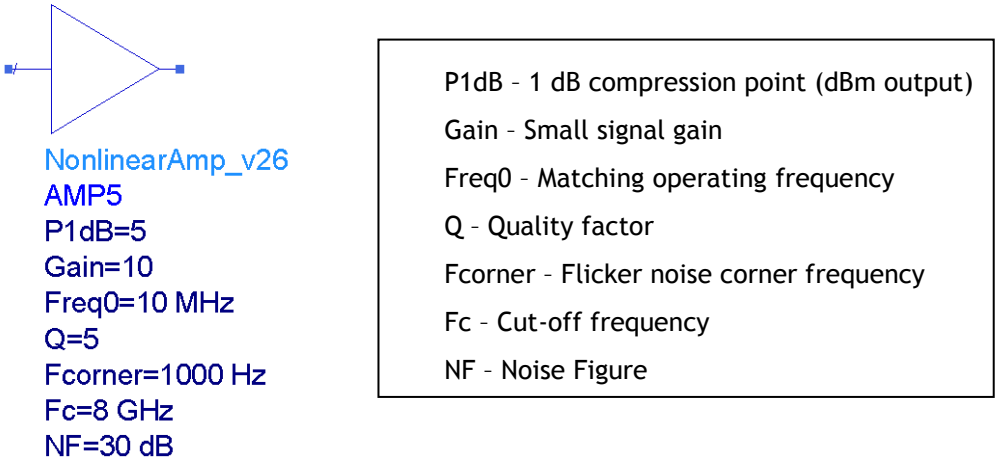

Figure 3.9 - ADS Amplifier model

The nonlinear power amplifier model is modelled by seven parameters as despicted in Figure 3.9. With these parameters our black box model will result in an amplifier with nonlinear response, given by 1dB compression point and Small signal gain. Frequency response given by the matching operating frequency, cut-off frequency and Q-factor. The phase noise response given by flicker noise corner frequency and noise figure.

Our model consists in 3 different blocks as we can see in Figure 3.10. At input and output we have matching blocks which give us the frequency response. In this case we have a perfectly matching circuit at 50 Ω. Then, between these two blocks, we have the nonlinearity response and phase noise response.

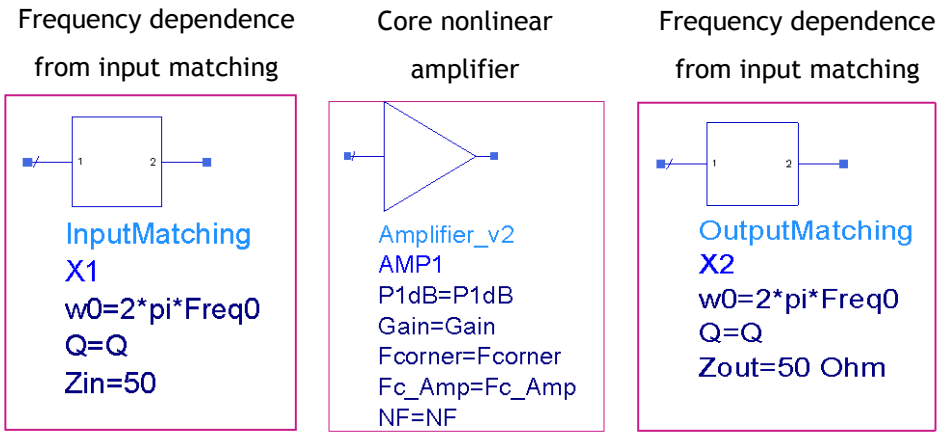

Figure 3.10 - Power amplifier modelling

Nonlinear System

We have a linear system if the output quantity is linearly proportional to the input as despicted, by dashed line, in Figure 3.11. In this case the gain, ratio between the output ant the input, is not affected by the input amplitude signal. Moreover, a nonlinear system is a system in which the output is a nonlinear function of the input (Solid line).

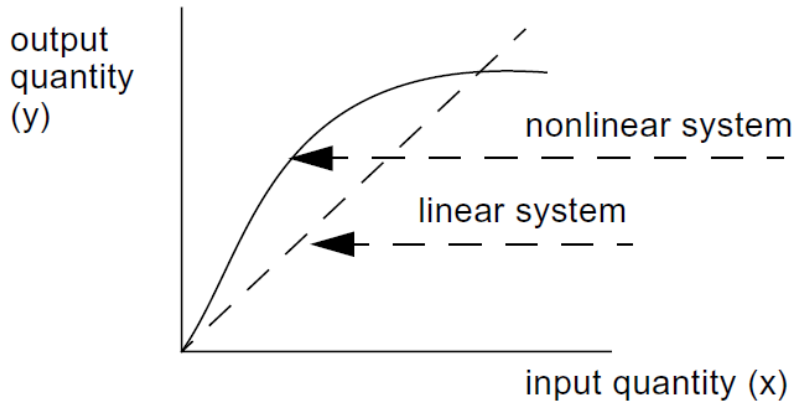

Figure 3.11 - Linear and Nonlinear system

The nonlinearty of the system can be modeled by polynomial model, which allows an easy calculation of spectral components. The output of the system can be described from a Taylor serie expansion

$$v_o = a_0 + a_1 v_i + a_2 v_i^2 + a_3 v_i^3 + \cdots + a_n v_i^n \qquad \text{Eq. 3.3.1}$$

Where a_0 to a_n are the real nonlinearity coefficients. Considering a single tone excitation

$$v_i = A\cos\omega_i t, \qquad \text{Eq. 3.3.2}$$

Substituting equation Eq. 3.3.2 into equation Eq. 3.3.1, an expression for v_o can be found (Considering only a 3rd-order behavior)

$$v_o = a_0 + a_1 A\cos\omega_i t + a_2 A^2\cos\omega_i t^2 + a_3 A^2\cos\omega_i t^3 \qquad \text{Eq. 3.3.3}$$

$$= \left(a_0 + \frac{1}{2}a_2 A^2\right) + (a_1 A + \frac{3}{4}a_3 A^3)\cos\omega_i t + \frac{1}{2}a_2 A^2\cos 2\omega_i t + \frac{1}{4}a_3 A^3\cos 3\omega_i t$$

The response consiste of a DC term and frequencies that are multiplies of the input frequency. Figure 3.12 shows us the unwanted frequency components introduced by harmonic distortion.

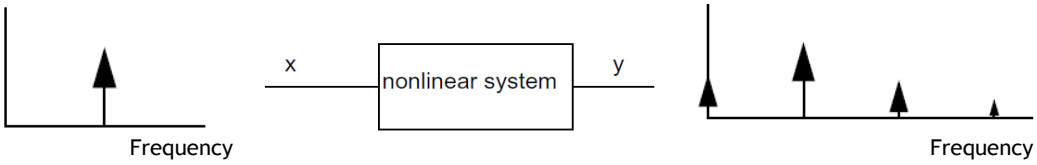

Figure 3.12 - Nonlinear effects

In our amplifier model we use hiperbolic tangent equation to give us the compression effect.

$$v_o = Vs\tanh(\frac{A_g v_i}{Vs}) \qquad \text{Eq. 3.3.4}$$

We can write the Taylor's series as

$$\tanh z = z - \frac{z^3}{3} + \frac{2z^5}{15} - \frac{17z^7}{315} + \cdots \qquad \text{Eq. 3.3.5}$$

Considering only a 3rd-order behavior

$$v_o = Vs(\frac{A_g v_i}{Vs} - \frac{\left(\frac{A_g v_i}{Vs}\right)^3}{3}) \qquad \text{Eq. 3.3.6}$$

$$= A_g v_i - \frac{A_g {v_i}^3}{3Vs^2}$$

$$= A_g A\cos\omega_i t - \frac{A_g A\cos\omega_i t^3}{3Vs^2}$$

$$= (A_g A - \frac{(A_g A)^3}{4Vs^2}) \cos \omega_i t - \frac{(A_g A)^3}{12Vs^2} \cos(3\omega_i t)$$

To obtain the non-linear gain, the above equation is divided by the input v_i,

$$Gain = \frac{v_o(\omega_i)}{v_i(\omega_i)} = \frac{a_1 A + a_3 A^3}{A} = a_1 + a_3 A^2, \qquad \text{Eq. 3.3.6}$$

Where $a_1 = A_g$ and $a_3 = \frac{(A_g)^3}{4Vs^2}$ then the small signal gain is A_g

The 1 dB gain compression point is given by (16)

$$P1dB = 10 \log \left(\frac{{a_1}^3}{a_3} \right) + 0.62\ dBm$$

$$P1dB = 10 \log(4Vs^2) + 0.62\ dBm \qquad \text{Eq. 3.3.7}$$

This two variables, Vs and A_g, control the gain and 1dB gain compression point giving us the nonlinearity characteristic, as despicted in Figure 3.13.

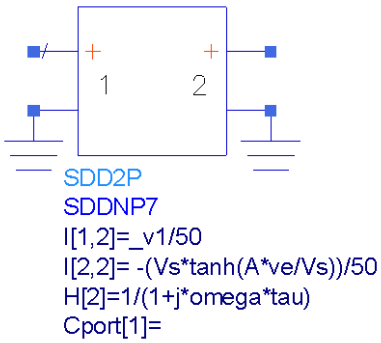

Figure 3.13 - SDD amplifier model

To understand better the SDD we can look to the equivalent circuit in Figure 3.14. For a matter of simplicity we work with 50 Ω in all model.

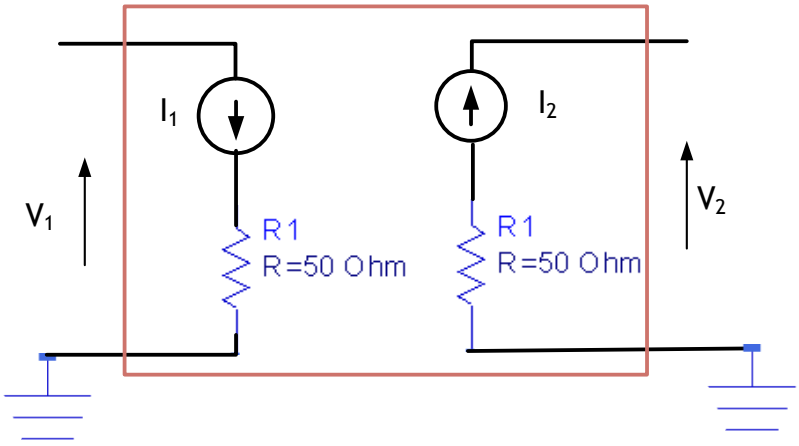

Figure 3.14 - SDD equivalent circuit

Both input and output current are using the weighting function to introduce cut-off frequency, Figure 3.15.

$$H[2] = \frac{1}{(1+j\omega\tau)},$$

where

$$\tau = \frac{1}{2\pi Fc}$$

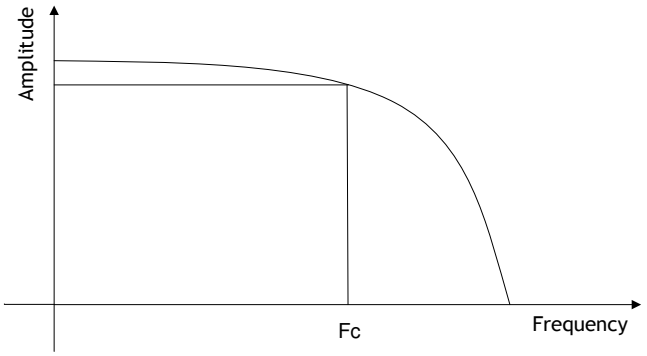

Figure 3.15 - Amplifier Cut-off frequency

The result of our model taking in account the gain compression is given in Figure 3.16. The output signal, on the blue line-1, show the gain saturation versus the input signal. We can see the gain versus the input on the red line-2 and the 1dB gain compression is given by the pink line-3.

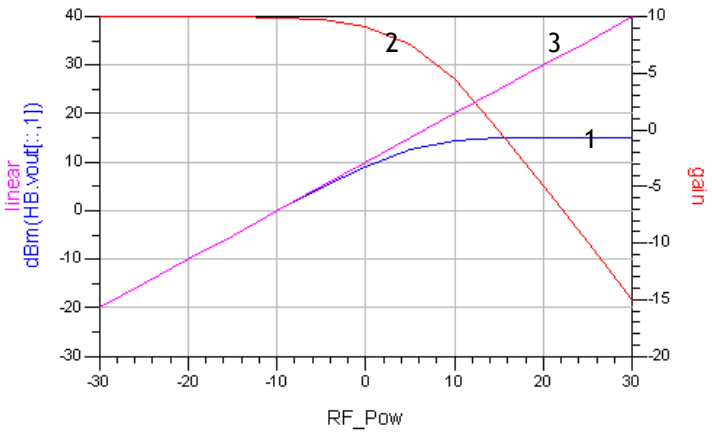

Figure 3.16 - Gain Compression result

Phase noise model

Taking the main expression of the amplifier phase noise we see that Noise Factor (F) is an important element

$$S_\varphi(f) = \frac{kTF}{P_0}(1 + f_c)\frac{1}{f},$$

The noise factor of a device specifies how much noise the device will add to the noise coming from the source.

When analyzing a circuit we transform the many possible sources of noise (generating noise currents and voltages) to an equivalent noise source at the input of the circuit as shown in Figure 3.17.

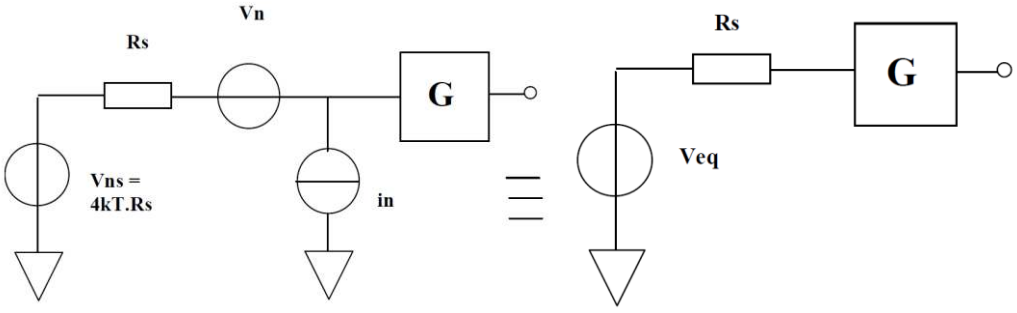

Figure 3.17 - Equivalent noise model

Vns- input noise power due to Rs

Rs – Source impedance

Vn – Voltage noise source

In – Corrent noise source

G- Amplifier Gain

Veq – Total equivalent input noise voltage

The $V_{eq}^2 = Vns^2 + Vn^2 + In^2Rs^2$ where $Vns = 4kTRs$

$$F = \frac{Total\ equivalent\ input\ noise\ power}{Input\ noise\ power\ due\ to\ the\ source\ only} = \frac{\mathrm{Vns}^2 + \mathrm{Vn}^2 + \mathrm{In}^2\mathrm{Rs}^2}{\mathrm{Vns}^2} = 1 + \frac{\mathrm{Vn}^2 + \mathrm{In}^2\mathrm{Rs}^2}{\mathrm{Vns}^2}$$

Noise Figure (NF) is the noise factor converted to dB,

$$NF = 10\log(F)\ dB$$

Then NF, given by voltage and current noise sources, will be a SDD parameter of our model which will give us the phase noise characteritic along with f_c.

Figure 3.18 - Voltage noise source, per sqrt(Hz)

The phase noise result in Figure 3.19 ($f_c = 1000\ Hz\ and\ NF = 30\ dB$)

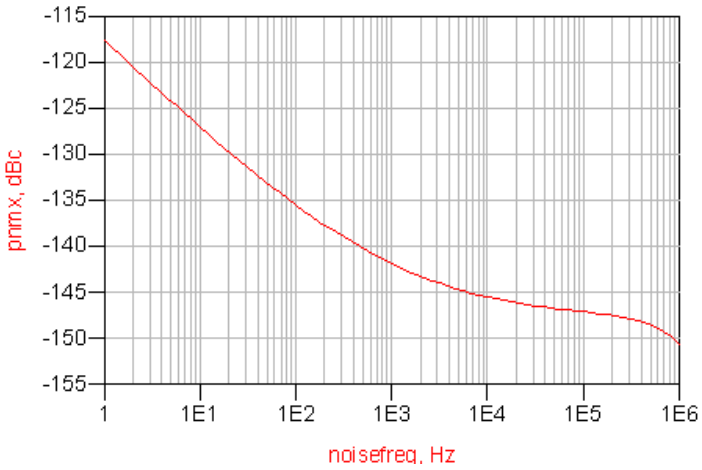

Figure 3.19 - Phase noise result

Frequency response

Here we try to do a input and output matching block this means that we can have a perfectly adapted 50 Ω amplifier at operating frequency, as despicted in Figure 3.21. Having the possibility to change input and ouput impedance, Zin, Zout, making a more realistic model.

Frequency dependence

from input matching

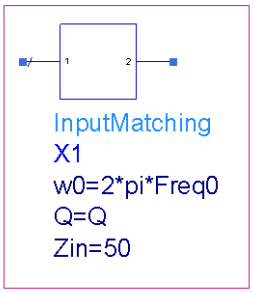

Figure 3.20 - Input matching using S2P-Eqn (ADS linear model)

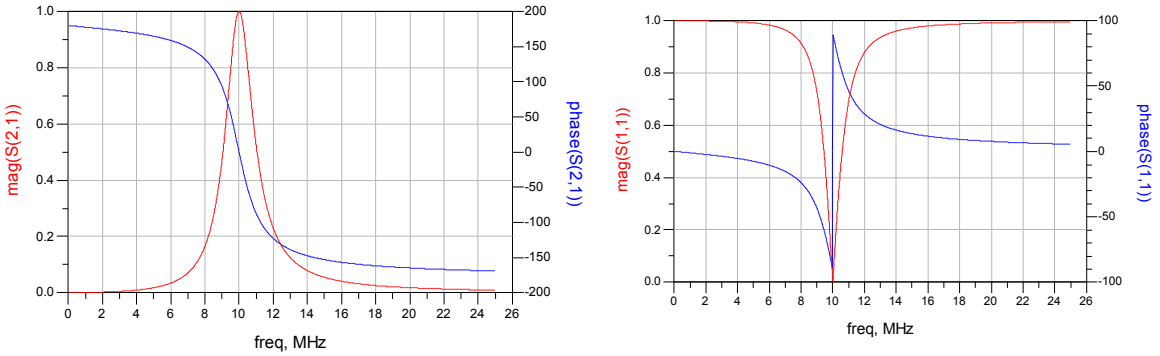

Figure 3.21 – S-Parameters (S21 in the left and S11 in the right)

An open loop Oscillator simulation was made to see if the Barkhausen condition has been met and as we can see in Figure 3.22.

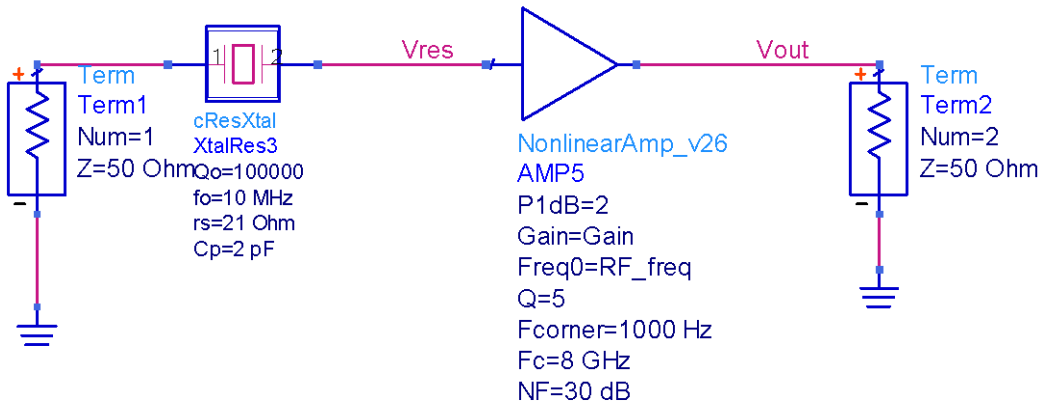

Figure 3.22 - Open Loop Crystal Oscillator

A crystal resonator was used, in fact, we use an electrical crystal model as depicted in Figure 3.23. Here the crystal resonator was not our main concern therefore we just use an example, in this case with a high-Q, 10^5. Figure 3.22 shows that at operating frequency ($arg[\beta A(j\omega)] = 0º$) we have a gain greater than the unity then barkhausen conditions are fulfilled.

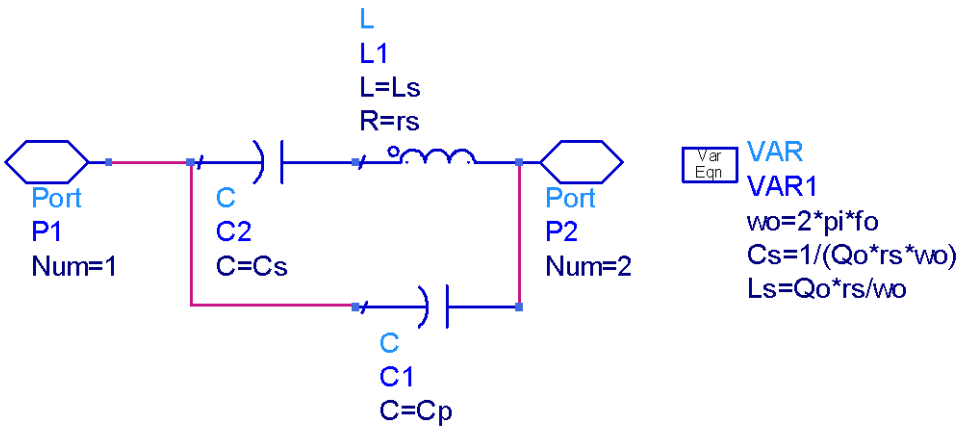

Figure 3.23 - Electrical crystal model

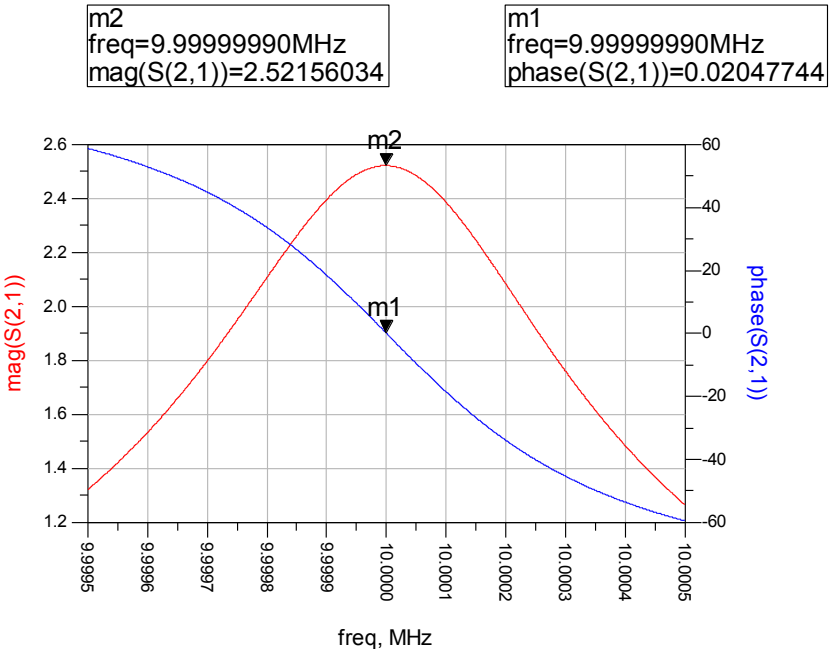

Figure 3.24 - Barkhausen conditions

Know doing a close loop to have a free running oscillator like Figure 3.25 we use to kind of simulation: OscPort simulation and AG simulation.

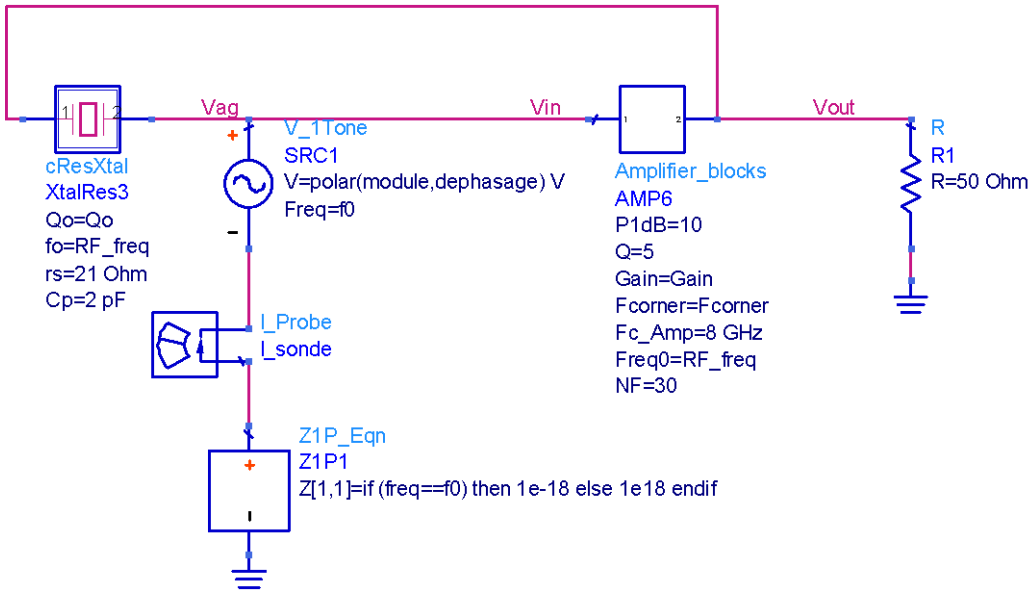

Figure 3.25 - Free Oscillator using AG Technique

We did the simulation using OscPort but as expected it does not work. We are in the presence of an autonomous circuit with a high-Q then we have convergence problems. From now we will only use AG technique in the oscillator simultion.

The result inFigure 3.26 shows the free running oscillator results using the AG technique. We can see the two main results from the left to the right: phase noise and the output spectrum. Then we have diferents parameters which are the inputs at the top and then parameters given by simulation. In the output spectrum result we an oscillation a 10.0000013MHz with a power of 11.4 dBm. At the phase noise result we can see the diference between the amplifier phase noise (solide line) and free oscillator phase noise. At frequencies below Leeson frequency (~2880 Hz) we see that the oscillator phase noise is multiplied by f^{-2} . Note that the models used so far have ignored the effect of the load. In this case we have 21Ω from crystal quartz resistor, 50 Ω output impedance of the amplifier and then 50 Ω loaded impedance. Therefore the oscillator phase noise is slightly higher than amplifier phase noise. An important conclusion is, as expected, in our model do not have even harmonics while using hiperbolic tangent for the nonlinearity approximation.

Inputs:

Gain	P1dB	Loaded Q	Noise Floor	Corner Freq.
10	10 dBm	1739	-160 dBc	1000 Hz

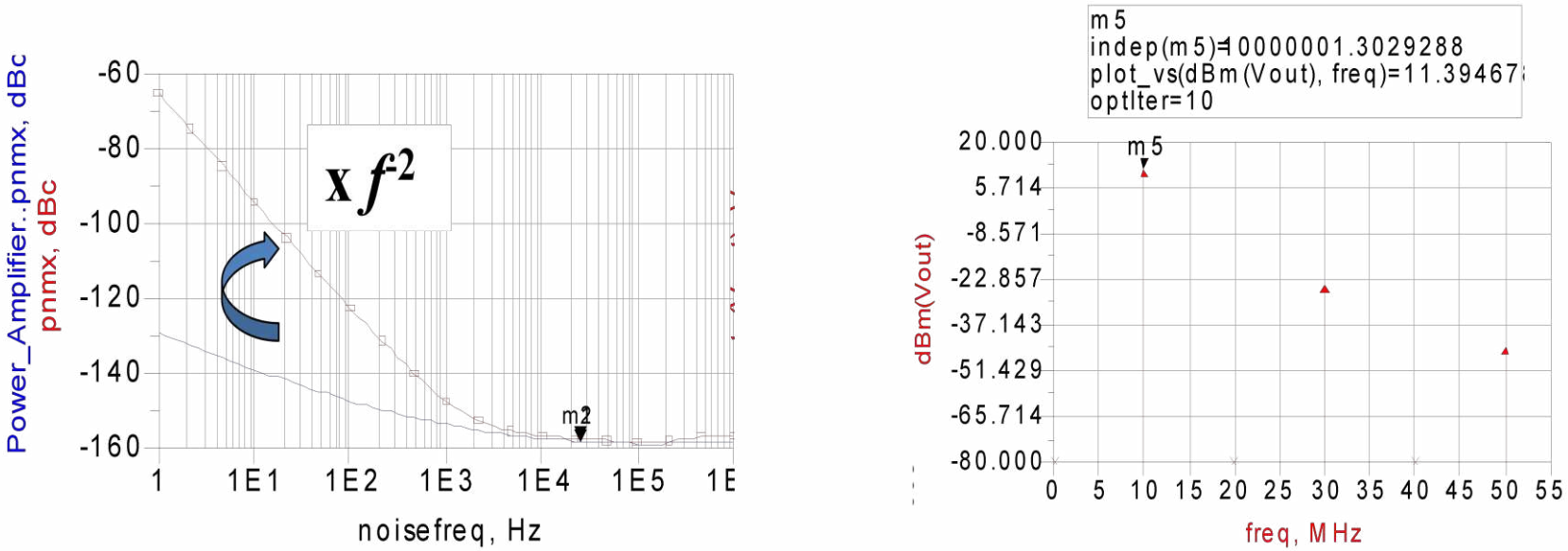

Results:

Leeson Freq.	Oscillation Freq.	Pin	Pout
2890.17 Hz	10000001.30 Hz	8.34 dBm	11.39 dBm

Figure 3.26 - Free Oscillator results using AG technique

Now let consider an Oscillator Injection using an injected signal with a phase noise characteristic as despicted in Figure 3.27

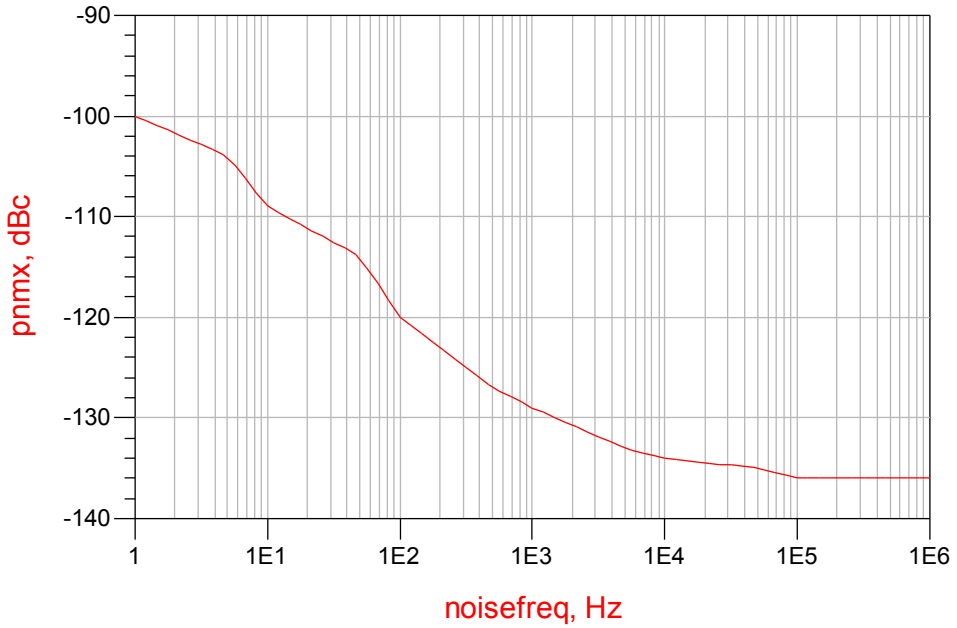

Figure 3.27 - Injected signal Phase Noise characteristic

As shown in Figure 3.28 the Kurakawa theory is confirmed. We inject a signal with -19dBm at 9.999991 MHz and with phase noise characteristic as shown in Figure 3.27. The parameter Delta_sync which is the diference between the free oscillator frequency and the injected oscillator frequency, gives us the shift in the oscillation frequency. We had 10.3 Hz (delta) of diference and now is ~0.04 Hz. The phase noise results (left) shows the injected phase noise signal (X line), free oscillator phase noise (solide line) and then the injected oscillator phase noise (square line). Here we see the synchronization between the two phase noises as said before.

Inputs:

Free oscillator	Leeson Freq.	Frequency
	2890.17 Hz	10000001.30 Hz

Injection	Power	Frequency	delta
	-19 dBm	9999991 Hz	10.3 Hz

Results:

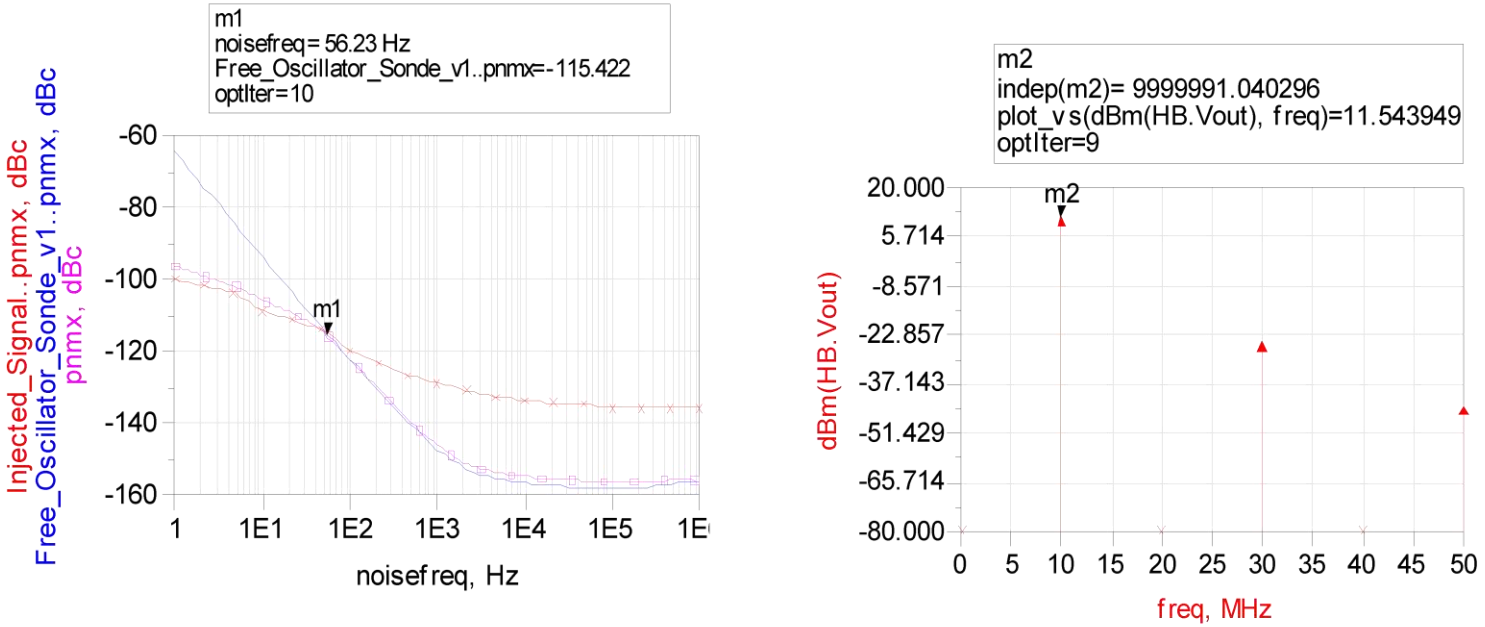

Oscillation Freq.	Delta_sync	Pin	Pout
9999991.04	0.04 Hz	8.60 dBm	11.54 dBm

Figure 3.28 - Injection oscillator simulation results

As we can see in Figure 3.29 the synchronisation between the injected phase noise (x line) and free oscillator phase noise (solide line) change with the level of injected power. With a low injected power we do not have synchronisation, with a big difference between the final frequency and the injected frquency (delta_sync). When we increase the injected power we increase Flock with delta_sync tending to zero. But with high P_{inj}, the injected phase noise start to have strong influence in the final phase noise. However these results were not expected from Kurokawa and Adler equations: in the first example with Pinj=-30 dBm we have Flock=12.2 which is above the delta=10.3 (f_o – f_{inj}) then we fulfill the locking condition Eq. 2.5.2 but we do not have lock frequency with delta_sync=6 Hz. With a high Pinj we can see the slight diference to the injected phase noise at low frequencies and the floor noise increases. One reason can be the use of empirical equations Eq. 2.5.3 and Eq. 2.5.4.

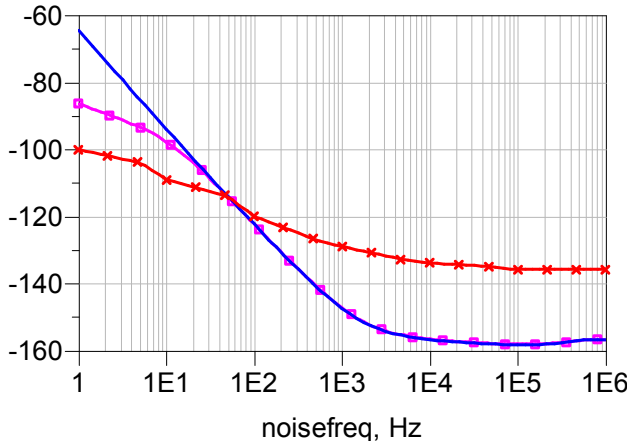

P_{inj}=-30 dBm
Delta_sync=6 Hz
F_{lock}= 12.2 Hz

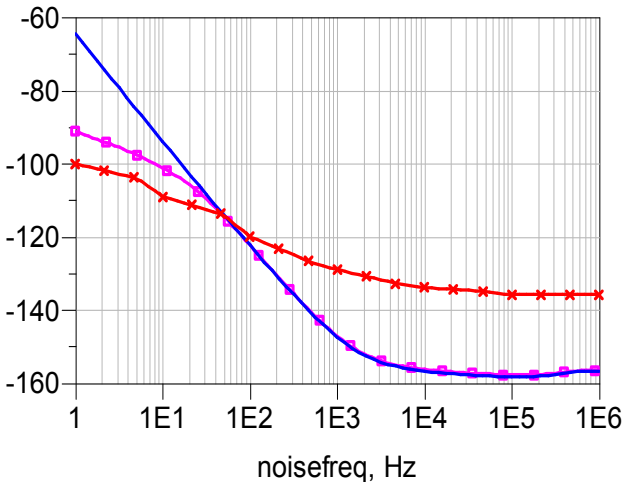

P_{inj}=-25 dBm
Delta_sync=2.7 Hz
F_{lock}= 21.7 Hz

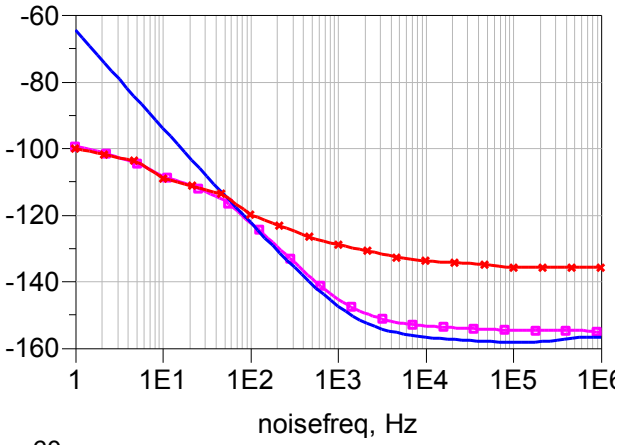

P_{inj}=-15 dBm

Delta_sync=-0.87 Hz

F_{lock}= 67 Hz

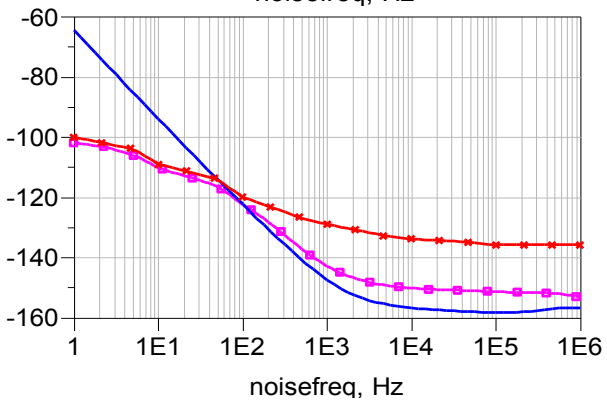

P_{inj}=-10 dBm

Delta_sync=-1.4 Hz

F_{lock}= 117 Hz

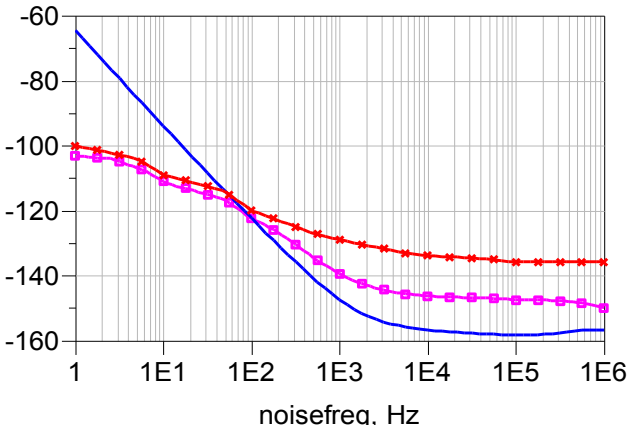

P_{inj}=-5 dBm

Delta_sync=-1.59 Hz

F_{lock}= 202 Hz

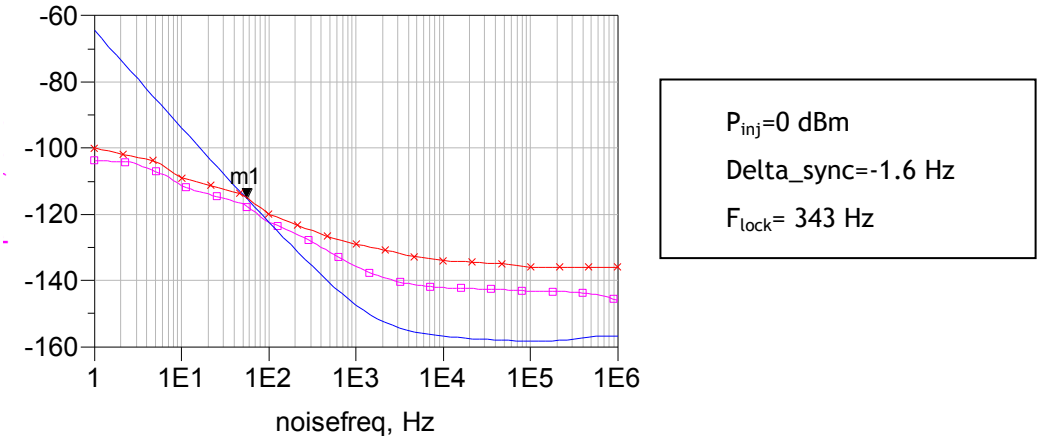

Figure 3.29 - Phase noise Injection results for different injected powers

Chapter 4

Injected Phototransistor Oscillator

The phototransistor combines detection and amplification functions in a device.

4.1 HPT Model

As we can see in Figure 4.1, a HPT has three ports, base, collector and common emitter, and an additional input –the Optical Input.

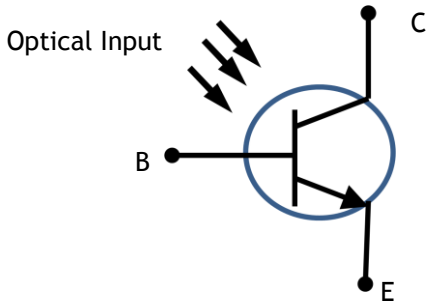

Figure 4.1 - HPT representation

The optical input is characterized by an amplitude modulated optical power signal (P_{opt}) which has two components:

$$P_{opt}(t) = P_{opt,DC} + P_{opt,RF}.\cos(\omega_{RF}.t + \varphi)$$

Where $P_{opt,DC}$ is optical DC component and $P_{opt,RF}$ is optical AC component. In our model we consider a purely electric behaviour representation. Then a current source represents the modulated optical signal. Basically we begin our representation after the detection module

working with an electrical signal characterized by one variable, P_{opt} which controls the photocurrent generator - I_{ph}.

$$I_{ph} = \frac{\alpha}{1 + j.\omega.(\frac{1}{2\pi F_{c,PD}})}.P_{opt} = r_{pd}.P_{opt}$$

Where α is the dc value of the r_{pd} short-circuit optical responsivity and $F_{c,PD}$ is the internal photodiode cut-off frequency (17).

The corresponding equivalent circuit is shown in Figure 4.2.

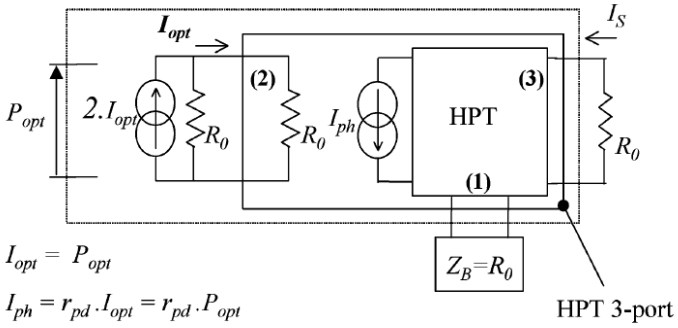

Figure 4.2 - Electric equivalent circuit of HPT

Our input optical current is given by

$$I_{opt} = \alpha_{c_A}.P_{opt}$$

Where α_{c_A} is the coefficient of homogeneity which we will consider equal to 1 A/W, then the optical input is represented by a 2. I_{opt} equivalent current source with two resistances R0. That means

$$I_{opt} = P_{opt}$$

This leads us to a HPT model with an input impedance of 50 Ω and a current source symbolically connected to a line without losses of 50 Ω. Then, we consider to have a perfectly adapted optical input which means no reflection from the HPT to the optical fiber.

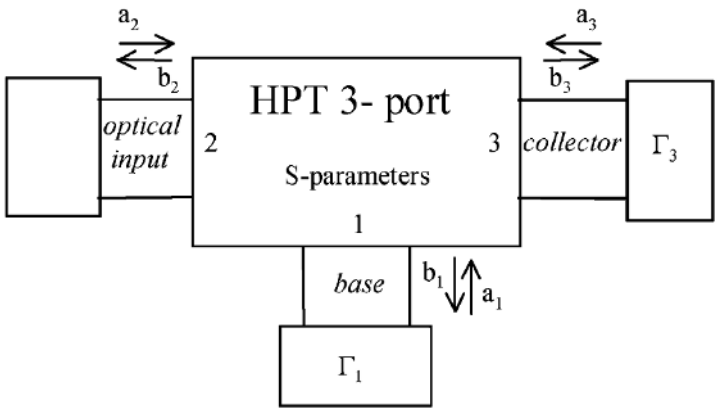

Figure 4.3 - Three-port scheme of the HPT

Considering the common-emitter configuration of a transistor we have a two port network between the base and the collector. With a phototransistor we can consider a three-port network, as shown in Figure 4.3. This model was proposed by Jean-Luc Polleux (18). It gives us a 9 terms opto-microwave S-parameter matrix, :

$$S = \begin{pmatrix} S_{11} & S_{12} & S_{13} \\ S_{21} & S_{22} & S_{23} \\ S_{31} & S_{32} & S_{33} \end{pmatrix}$$

Port 2 is the optical input where a2 and b2 are the incident and reflected power waves. Port 1 and port 3 are the electrical port base-emitter and collector-emitter, respectively. On one side we have the typical two-port electrical s-parameters: S_{11}, S_{13}, S_{31}, S_{33}. On the other side we have opto-microwave s-parameters of the phototransistor: S_{21}, S_{22}, S_{23}, S_{12}, S_{32}. We already said that there is no reflection from the optical interface. This means that we b2 is fixed at zero, therefore, S22=S21=S23=0. Then, as we can see

$$S = \begin{pmatrix} \boxed{S_{11}} & S_{12} & \boxed{S_{13}} \\ 0 & 0 & 0 \\ \boxed{S_{31}} & S_{32} & \boxed{S_{33}} \end{pmatrix}$$

we just have two opto-microwave s-parameters: S_{12} and S_{32} which represents the opto-microwave gain transfer from the optical input to the base and collector electrical ports, respectively.

It is possible to write the transducer power gain G_T using 50 Ω base/collector impedance,

$$G_T = |S_{32}|^2 = \frac{\frac{1}{2}.R_0.I_S^2}{\frac{1}{2}.R_0.I_{opt}^2} = \frac{I_S^2}{I_{opt}^2} = \frac{I_S^2}{P_{opt}^2}$$

If matching network are added on the based and collector, two important factors are to be considered, see (18).

4.2 HPT simulation Model

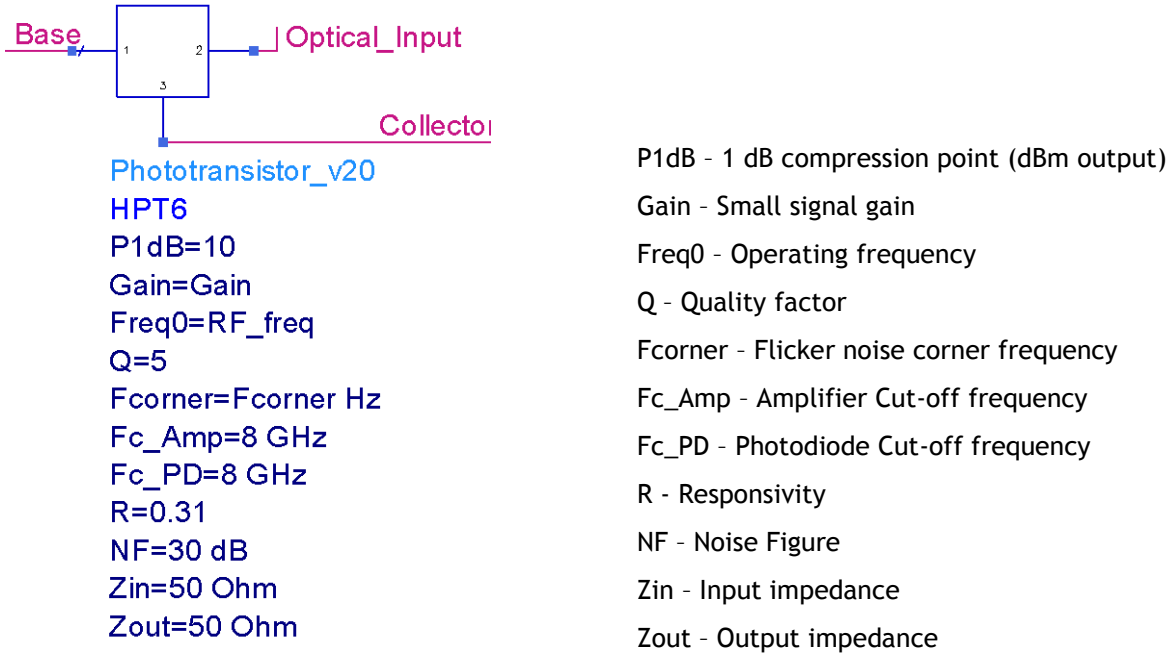

Figure 4.4 - HPT ADS model

As we can see in Figure 4.4 a few parameters were added: photodiode Cut-off frequency, responsivity, input and output impedance. Inside our model we have four blocks as despicted in Figure 4.5. Detector block play the role of the optical input characterized by its frequency (Fc_PD) response and responsivity (R).

Frequency dependence from the input matching | **Detector Block** | **Core nonlinear Amplifier** | **Frequency dependence from the output matching**

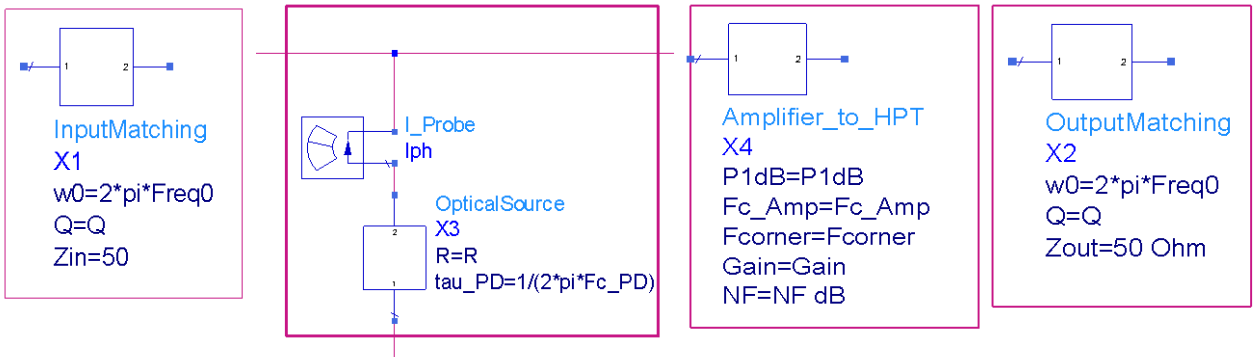

Figure 4.5 - HPT Modelling

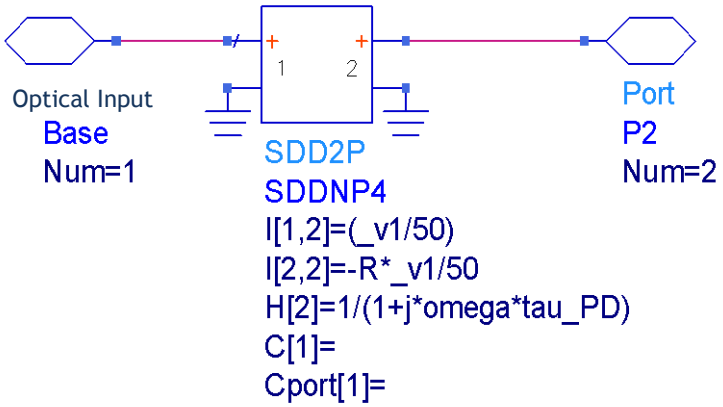

Figure 4.6 - Optical source SDD

Figure 4.7 shows the opto-microwave gain transfer from the optical input to the collector when a R=0.5 is used.

$$(S32)_{dB}=(S21)_{dB} + 10 \log (R^2)= 10 \text{ dB} - 10 \log (0.5^2)= 3.9794 \text{ dB}$$

This result in confirmed at Figure 4.7.

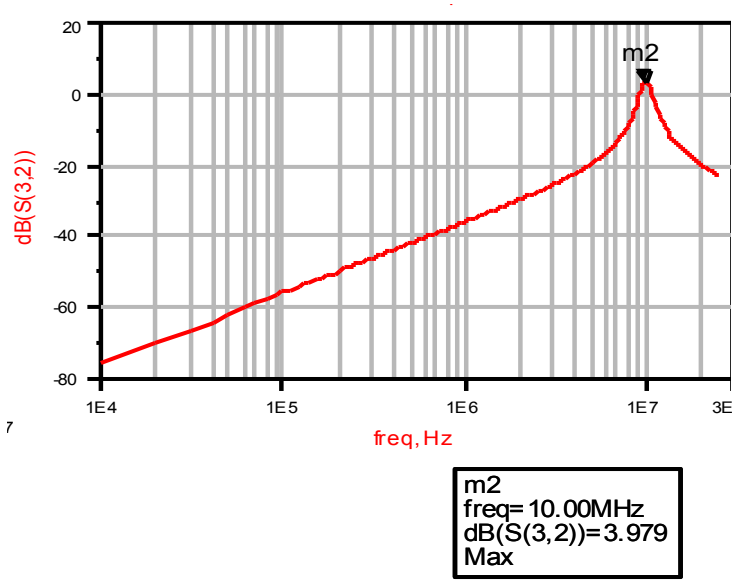

Figure 4.7 - Opto-microwave gain transfer from the optical input to the collector electrical port

4.3 HPT Oscillator Simulations

Free HPT Oscillator was made and like expected we get the same results as the free injected oscillator, Figure 4.8. In the case of the Injected Phototransistor Oscillator, Figure 4.9, the simulation was not complete, but we espect the same result as well. The only difference is the injection which now comes from the optical input using a voltage controlled source.

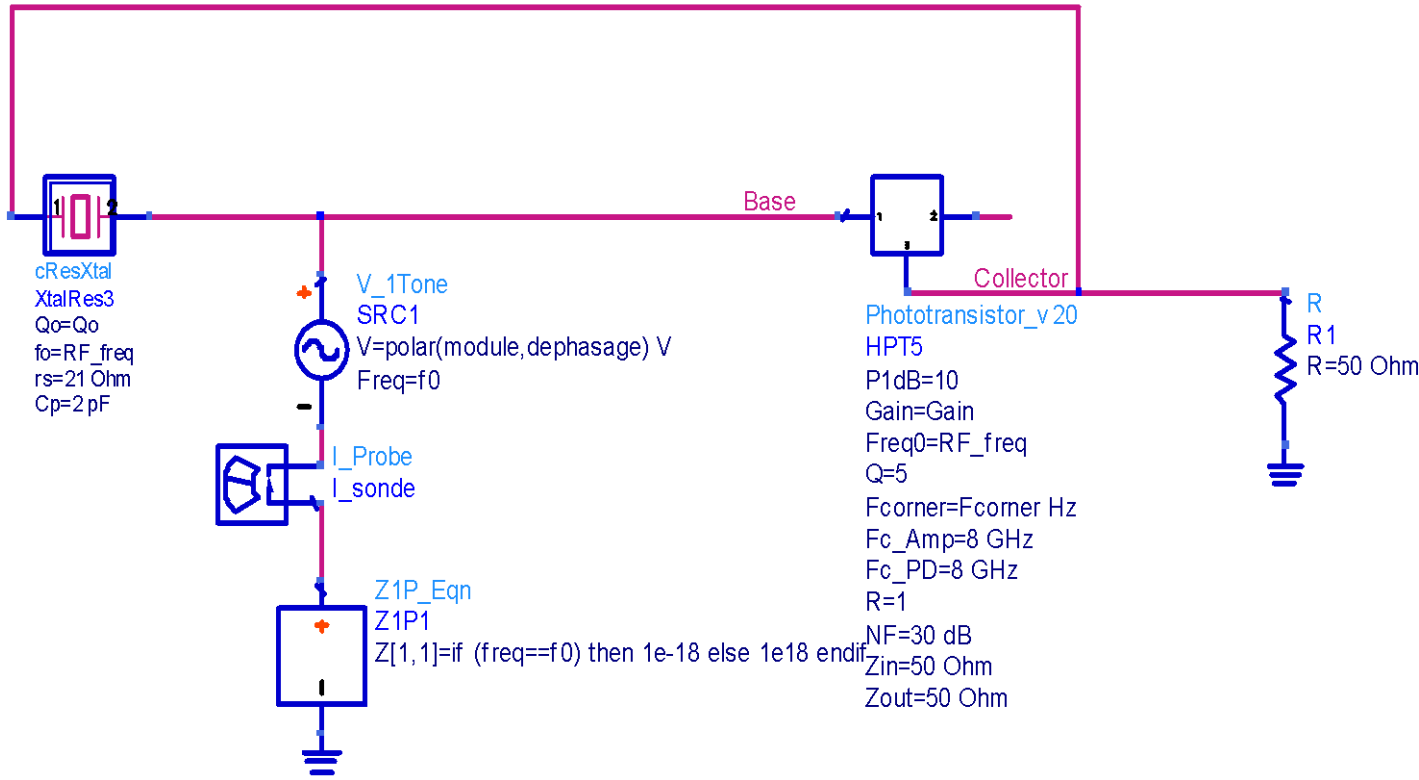

Figure 4.8 - Free Injected Phototransistor Oscillator

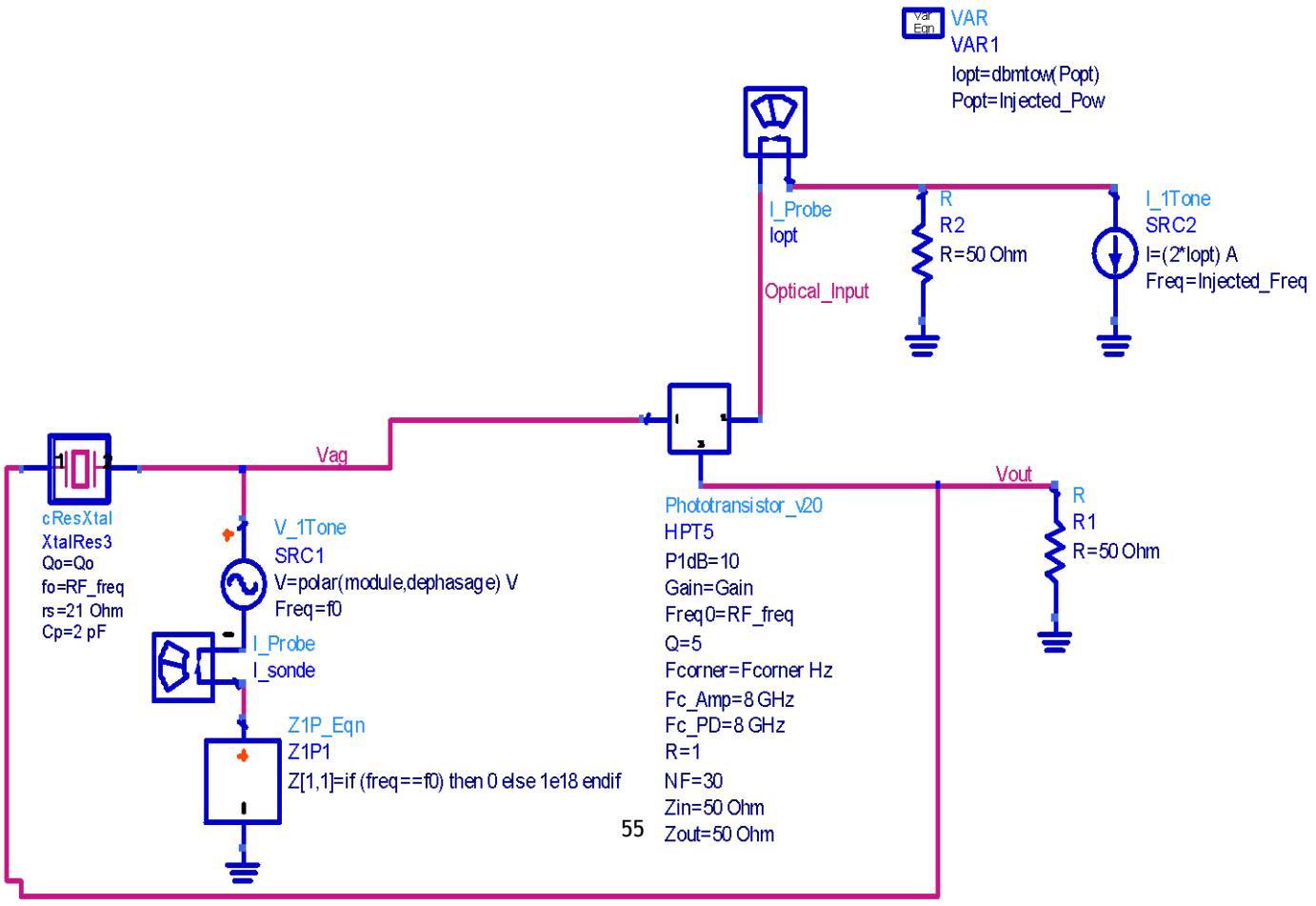

Figure 4.9 - Injected Phototransistor Oscillator

Chapter 5

Conclusions and Perspectives

A Nonlinear Power Amplifier was developed using ADS software considering phase noise, frequency response and nonlinearities characteristics. Its validity was proved using the Power amplifier into the Oscillator where Leeson model were visualized. Auxiliary Generator technique was presented for autonomous and synchronized circuit's simulation using Harmonic Balance. Oscillator Injection was demonstrated using our PA model where kurokawa model was proved even if slight discrepancies to the simulation were revelled. HPT model was presented were the optical input was modulated by a current controlled source.

The validation of the injected phototransistor oscillator is not complete. So next step is to finish this point. Comparison between simulations, theory and measurements have to be done since we found some differences which tell us that the empirical equations may not be complete; Find the best characteristics of the HPT model changing the different parameters and design an electric circuit to implement Oscillator Injection.

References

1. **Leeson, D.B.** "Simple model of feedback oscillator noise spectrum". Proc. IEEE, Feb. 1966, p. 329.

2. **Kurokawa, K.** "Noise in synchronized oscillators", IEEE Transc. on microwave theory and techniques, vol. mtt-16, no. 4, april 1968.

3. *Phase Noise Characterization of Microwave Oscillators, Frequency Discriminator Method, Product Note 11729C-2, Hewlett-Packard, California.*

4. **Rubiola, Enrico.** *"Phase Noise and Frequency Stability in Oscillators".* s.l. : Cambridge University Press, 2008. ISBN 978-0-521-88677-2.

5. **R.Adler.** "A study of locking phenomena in oscillators". Proc. IEEE, 1973, Vol. 61, pp. 1380-1385.

6. **X. Huang, F. Tan,W. Wei, W. Fu.** "A Revisit To Phase Noise Model Of Leeson", IEEE Freq. control symp., 2007.

7. **U. L. Rohde, A. K. Poddar.** "Mode-Selection and Mode-Feedback Techniques Optimizes VCXO Performances", IEEE Sarnoff Symposium, 2008.

8. **S.-H. Zhou, J.-P. Zeng, Q. Xiong, Y. Zeng.** "Study and Design of Integrated Crystal Oscillator", IEEE International conference on wireless, 2009.

9. **J. Everard, K. Ng.** "Ultra-Low Phase Noise Crystal Oscillators", IEEE Freq. control symp., 2007.

10. **X. Ou, W. Zhou, H. Kang.** "Phase-noise Analysis for single and Dual-mode Colpitts Crystal Oscillators", IEEE int. freq. control symp., 2006.

11. **Y. WATANABE, S. KOMINE, S. GOKA, H. SEKIMOTO, T. UCHIDA.** "Near-Carrier Phase-Noise Characteristics of NarrowBand Colpitts Oscillators", IEEE International Ultrasonics, Ferroelectrics and Frequency Control, 2004.

12. **T. Uchida, M. Koyama, Y. Watanable, H. Sekimoto.** "A low phase-noise oscillator design for high stability OCXOS", IEEE International FrequencyControl Symp (1996).

13. **A. Suárez, R. Quéré.** *"Stability Analysis ofNonlinear Microwave Circuits",*. s.l. : ARTECH HOUSE, INC, 2003. ISBN 1-58053-303-5.

14. **Verspecht, J.** "Black Box Modelling of Power Transistors in the FrequencyDomain", Hewlett-Packard Network Measurement and Description Group, 1996.

15. **H. Taher, D. Schreurs, B. Nauwelaers.** "Black Box Modelling at the Circuit level:Op-Amp as a Case Study", IEEE Electrotechnical conference, 2006.

16. **Baudoin, G.** *Radiocommunications numerique, Tome1: Principes, modélisation et simulation, Dunod Electronique, 2002.*

17. **J.L. Polleux, L. Paszkiewicz, A.L. Billabert, J. Salset, C. Rumelhard.** "Optimization of InP–InGaAs HPT Gain: Design of anOpto-Microwave Monolithic Amplifier", IEEE Transactions on microwave theory and techniques, vol. 52, no. 3, march 2004.

18. **Polleux, J.L.** "Contribution à l'étude et à la modélisationde phototransistors bipolaires à hétérojonctionSiGe/Si pour les applications opto-microondes". Ph D thesis, CNAM, Paris, Oct. 2001.

19. **G, Sauvage.** "Phase noise in oscillators: A mathématical analysis of Leeson's model", IEEE Transactions on Instrumentation and Measument, vol.I.M.-26, N°4 December 1977.

20. **D. A. Teeter, J.R East, R.K. Mains, G.I. Haddad.** "Large-Signal Numerical and Analytical HBT Models", IEEE Trans. Electron Devices, vol. 40, no. 5, pp. 837-845, 1993.

21. **R. Brendel, G. Maranneau, T. Blin, M. Brunet.** "Computer aided design of quartz oscillators", IEEE Transc. on ultrasonics, ferroelectrics and freq. control, vol. 42, no. 4, july 1995.

22. **F.L. Walls, J.R. Vig.** "Fundamental limits of the frequency stabilities of crystal oscillators", IEEE Transc. on ultrasonics,ferroelectrics and freq. control, vol. 42, no. 4, july 1995.

23. **Y. Watanable, H. Sekimoto, S. Goka, I. Niimi.** "A dual mode oscillator basedo n narrow-bandcrystal oscillators with resonator filters ",IEEE International FrequencyControl Symp (1997).

24. **A. Suárez, J. Morales, R. Quéré.** "Synchronization Analysis of AutonomousMicrowave Circuits Using NewGlobal-Stability Analysis Tools", IEEE Transc. on microwave theory and techniques, vol. 46, no. 5, may 1998 .

25. **M. Addouche, R. Brendel, D. Gillet, N. Ratier, F. Lardet-Vieudrin, J. Delporte.** "Modeling of Quartz Crystal Oscillators by Using Nonlinear Dipolar Method",IEEE Transc. on ultrasonics, ferroelectrics, and freq. control, vol. 50. no. 5 , may 2003 .

26. **S. Galliou, F. Sthal, M. Mourey.** "New Phase-Noise Model for CrystalOscillators: Application to the Clapp Oscillator", IEEE Transc. on ultrasonics, ferroelectrics, and freq. control, vol. 50, no. 11, november 2003.

27. **A. Hati, D. A. Howe, F. L. Walls, D. Walker,.** "Noise Figure vs. PM Noise Measurements: A Study at Microwave Frequencies",Proc. IEEE Freq. Contr. Symp., 1993.

28. **F. Ramírez, M. Elena de Cos, A. Suárez.** "Nonlinear Analysis Tools for the Optimized Designof Harmonic-Injection Dividers", IEEE Transc on microwave theory and techniques, vol. 51, no. 6, june 2003.

29. **H. Martinez-Reyes, G. Quadri, T. Parenty, C. Gonzalez, B. Benazet, O. Llopis.** "Optically Synchronized Oscillators for Low PhaseNoise Microwave and RF Frequency Distribution", IEEE Microwave conference, 2003.

30. **Chang, Heng-Chia.** "Phase Noise in Self-Injection-LockedOscillators—Theory and Experiment", IEEE Transc. on microwave theory and techniques, vol. 51, no. 9, september 2003.

31. **Razavi, B.** "A Study of Injection Locking and Pullingin Oscillators", IEEE JOURNAL OF SOLID-STATE CIRCUITS, VOL. 39, NO. 9, SEPTEMBER 2004.

32. **E. Shumakher, G. Eisenstein.** "Noise Properties of Harmonically Injection-Locked Oscillators", IEEE PHOTONICS TECHNOLOGY LETTERS, VOL. 16, NO. 3, MARCH 2004.

33. **J. van Beek, P. Steeneken, B. Giesbers.** "A 10MHz piezoresistive MEMS resonator with high Q", IEEE Int. freq. control symp., 2006.

34. **X. Duan, K. Mayaram.** "Robust Simulation of High-Q Oscillators Using aHomotopy-Based Harmonic Balance Method", IEEE TRANSACTIONS ON cad OF INTEGRATED CIRCUITS AND SYSTEMS, VOL. 25, NO. 12, DECEMBER 2006.

35. **T. Adachi, D. Akamatsu, K. Hirama, Y. Nakagawa, T. Yanagisawa.** "A Dual-T Quartz Crystal Resonator Circuit and itsApplication to 10MHz Oscillator", IEEE Freq. control symp., 2008.

36. **Evarard, J.** "Low Phase Noise Oscillators: Theory and Application", IEEE Freq. control symp., 2009.